

SURFACE ENGINEERING OF STAINLESS STEELS

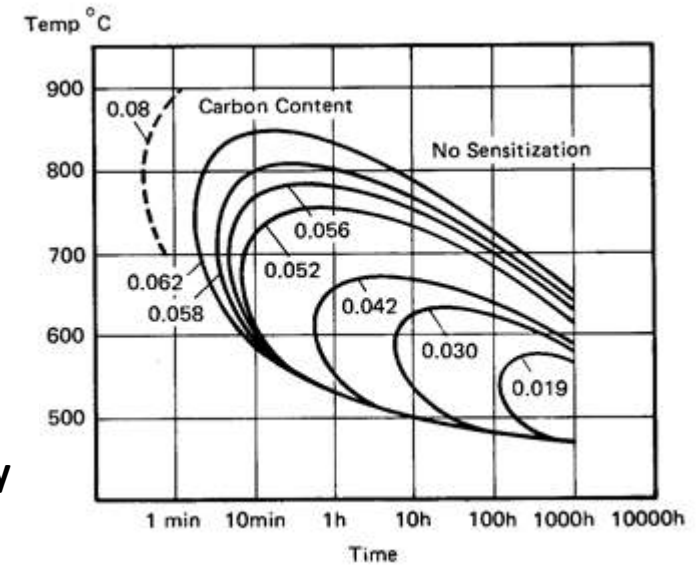
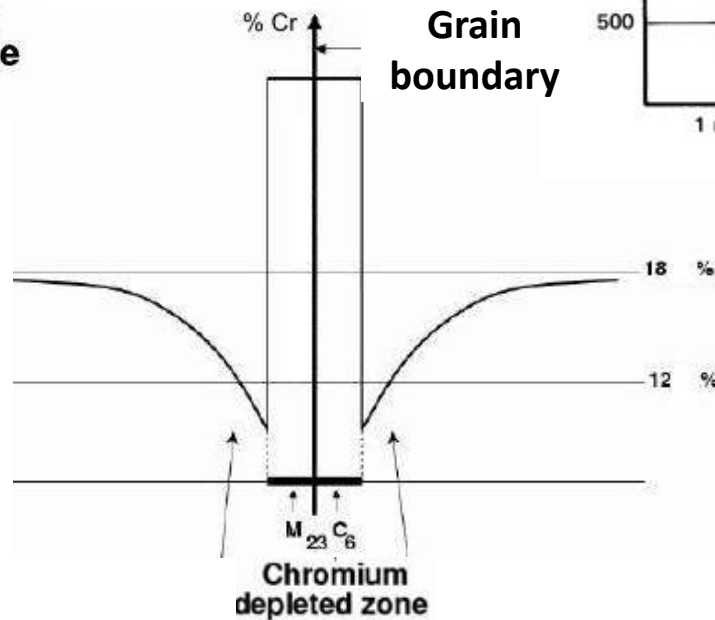
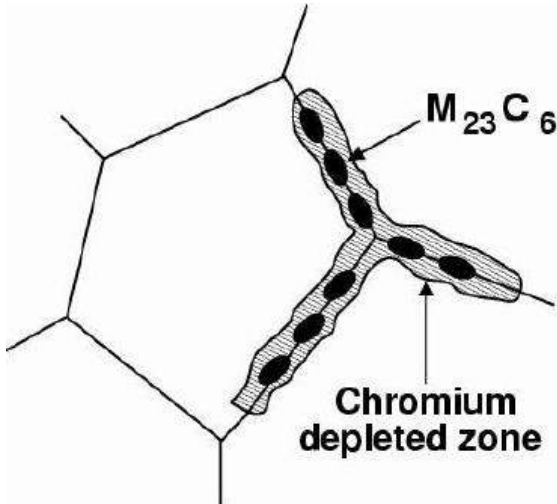
André Paulo Tschiptschin

Metallurgical and Materials Engineering Department
University of São Paulo

- Austenitic (ASS), Martensitic (MSS), Duplex (DSS) and Precipitation Hardening (PH) stainless steels have been used in a variety of applications within the refining and petrochemical industry, where high corrosion resistance and mechanical properties are required.
- Surface properties of these materials may be improved by thermochemical and plasma assisted treatments, to reach better performance in highly stressed tribological systems.
- Thermochemical and plasma assisted surface treatments have been proposed to improve tribological properties of these CRA.
 - HTGN \Rightarrow High Temperature Gas Nitriding
 - LTGN \Rightarrow Low Temperature Gas Nitriding
 - LTPN \Rightarrow Low Temperature Plasma Nitriding
 - LTPC \Rightarrow Low Temperature Plasma Carburizing
 - LTPNC \Rightarrow Low Temperature Plasma Nitrocarburizing

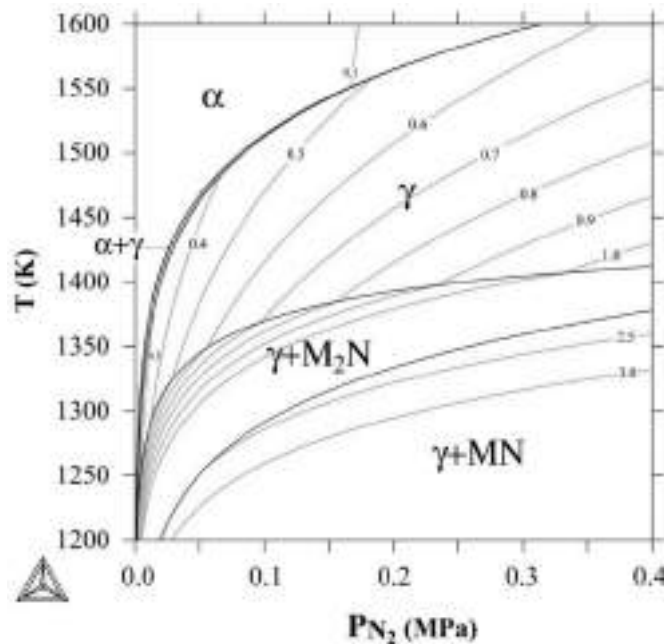
- The common characteristic of these surface treatments is the introduction of nitrogen or carbon in solid solution by diffusional processes, increasing hardness and developing compressive residual stresses, as well.
- Increasing carbon or nitrogen contents in solid solution in austenite, up to and also beyond the solid solubility limit, increases steadily the hardness of these alloys.
- Chromium nitrides or chromium carbides precipitation should be avoided in order to avoid sensitization and preserve corrosion resistance.
- High Temperature Gas Nitriding allows obtaining equilibrium nitrogen contents, up to 1.1 wt.%, in solid solution in austenite, depending on SS chemical composition, N_2 potential in the nitriding atmosphere, nitriding temperature and pressure.

Improve surface hardness without loss of corrosion resistance



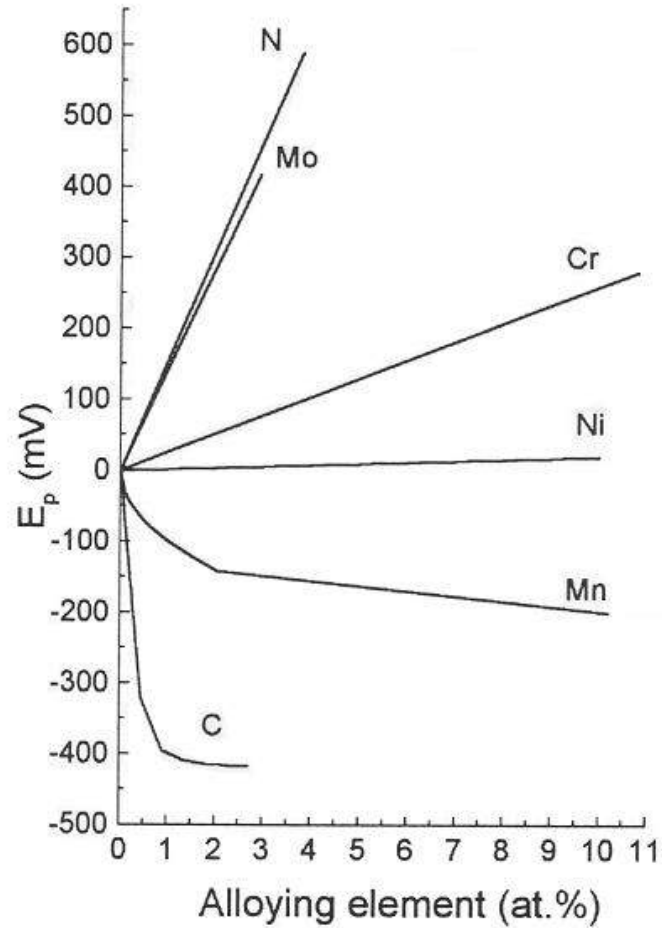
$Cr_{23}C_6$ precipitation harms the corrosion resistance due to Chromium depletion (sensitization)

- High Temperature Gas Nitriding \Rightarrow equilibrium nitrogen contents, up to 1.1 wt.%, in solid solution in austenite.
- Solid-state nitrogen alloying technique, consisting of exposing SS to a N_2 -containing gas atmosphere in the range 1000-1200°C.



Phase fields and nitrogen iso-concentration lines for a Fe-16.2 wt% Cr alloy

- Atomic nitrogen is interstitially absorbed at the surface of the steel and then diffuses into the near surface region, promoting hardening and improving corrosion resistance.



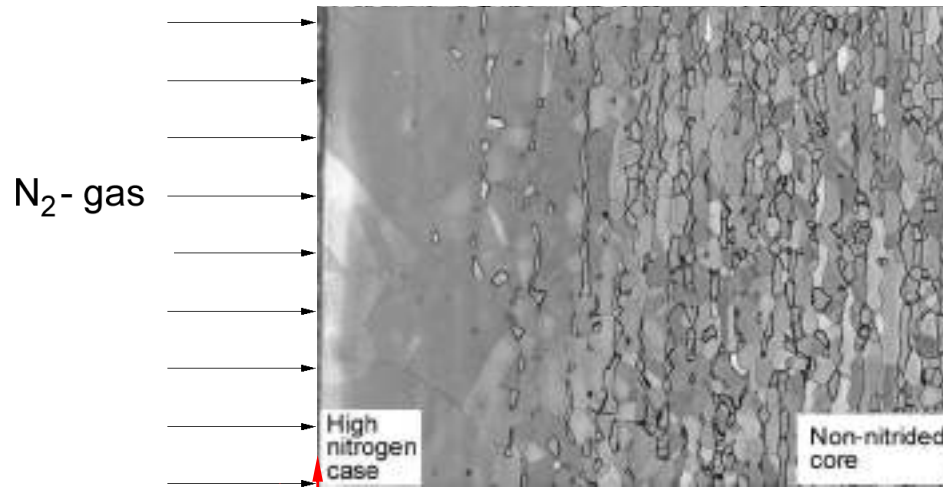
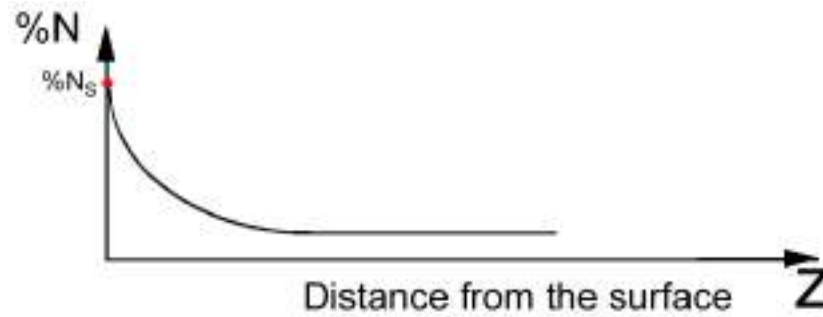
- Change in pitting potential of 18 wt% Cr austenitic stainless steels in dilute chloride solution [Speidel, 1991]

- Stainless Steels:

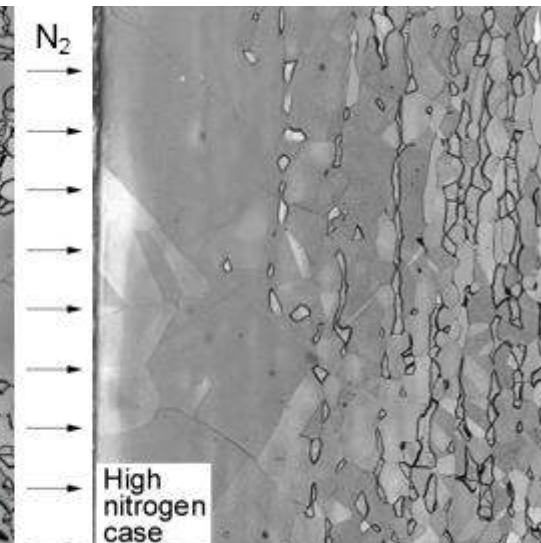
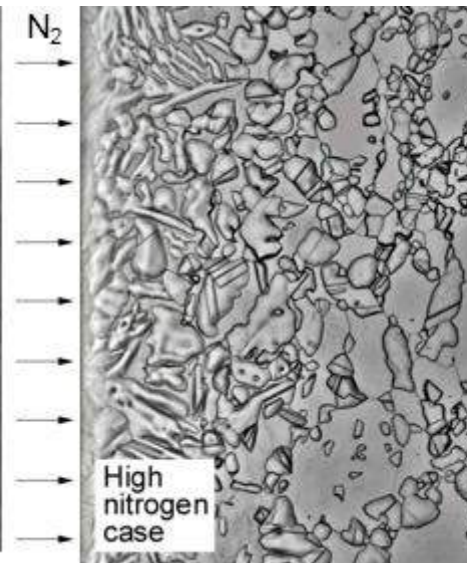
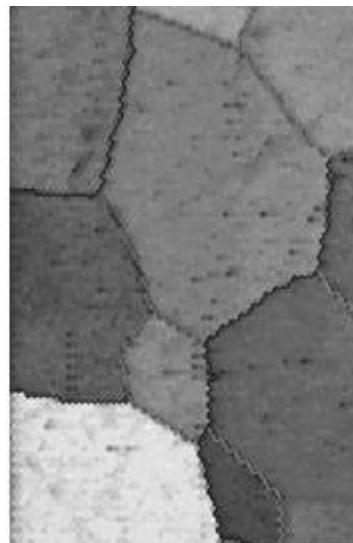
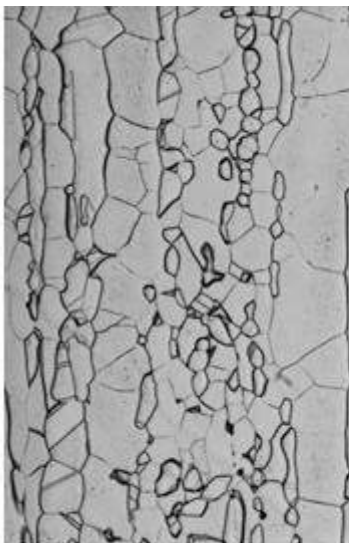
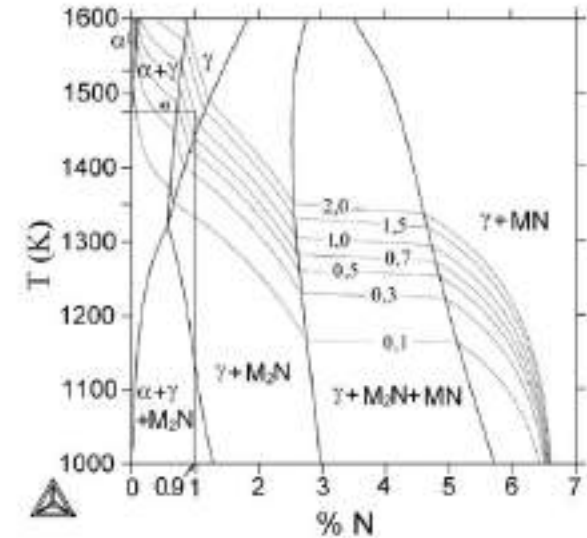
- HTGN Duplex SS \Rightarrow fully austenitic layer \uparrow % N
- HTGN Dual phase ($\alpha + M$) \Rightarrow fully martensitic layer \uparrow % N
- HTGN martensitic SS \Rightarrow fully martensitic layer \uparrow % N
- HTGN austenitic SS \Rightarrow fully austenitic layer \uparrow % N

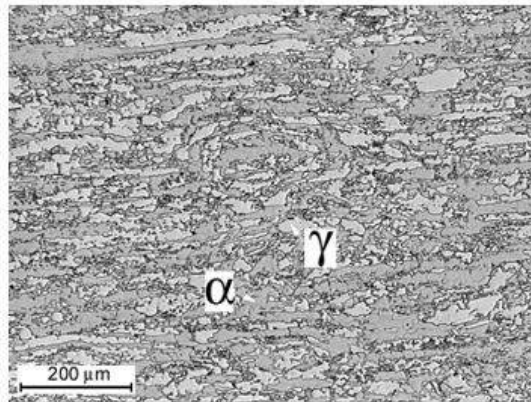
- Properties:

- High Hardness (martensitic) \Rightarrow Roller bearings and tools.
- Wear resistance (Cavitation-erosion, Erosion-corrosion) \Rightarrow pump rotors slurry environments.
- Corrosion resistance (generalized and localized) \Rightarrow surgical implants, biomedical application, retaining rings, etc.

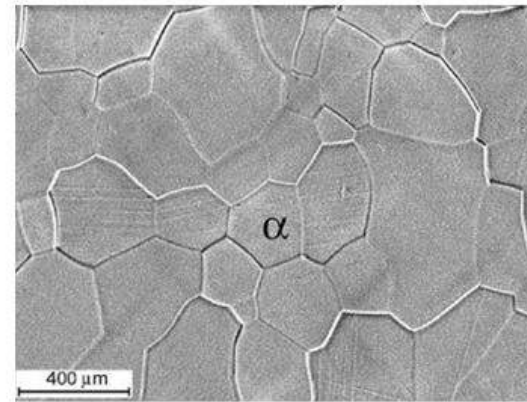


- When UNS S31803 duplex stainless steel is heated at 1200°C for HTGN the structure becomes completely ferritic.
- During nitriding ferrite transforms to Widmanstätten austenite.
- At the end a fully austenitic case is achieved

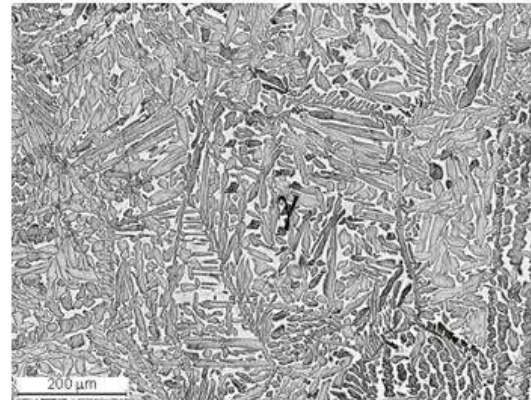




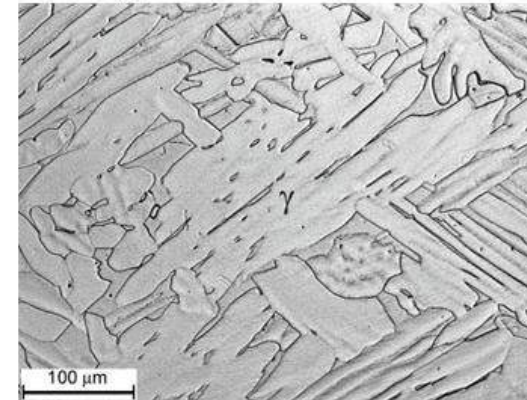
(a) Hot rolled



(b) 1150 ° C vacuum heated

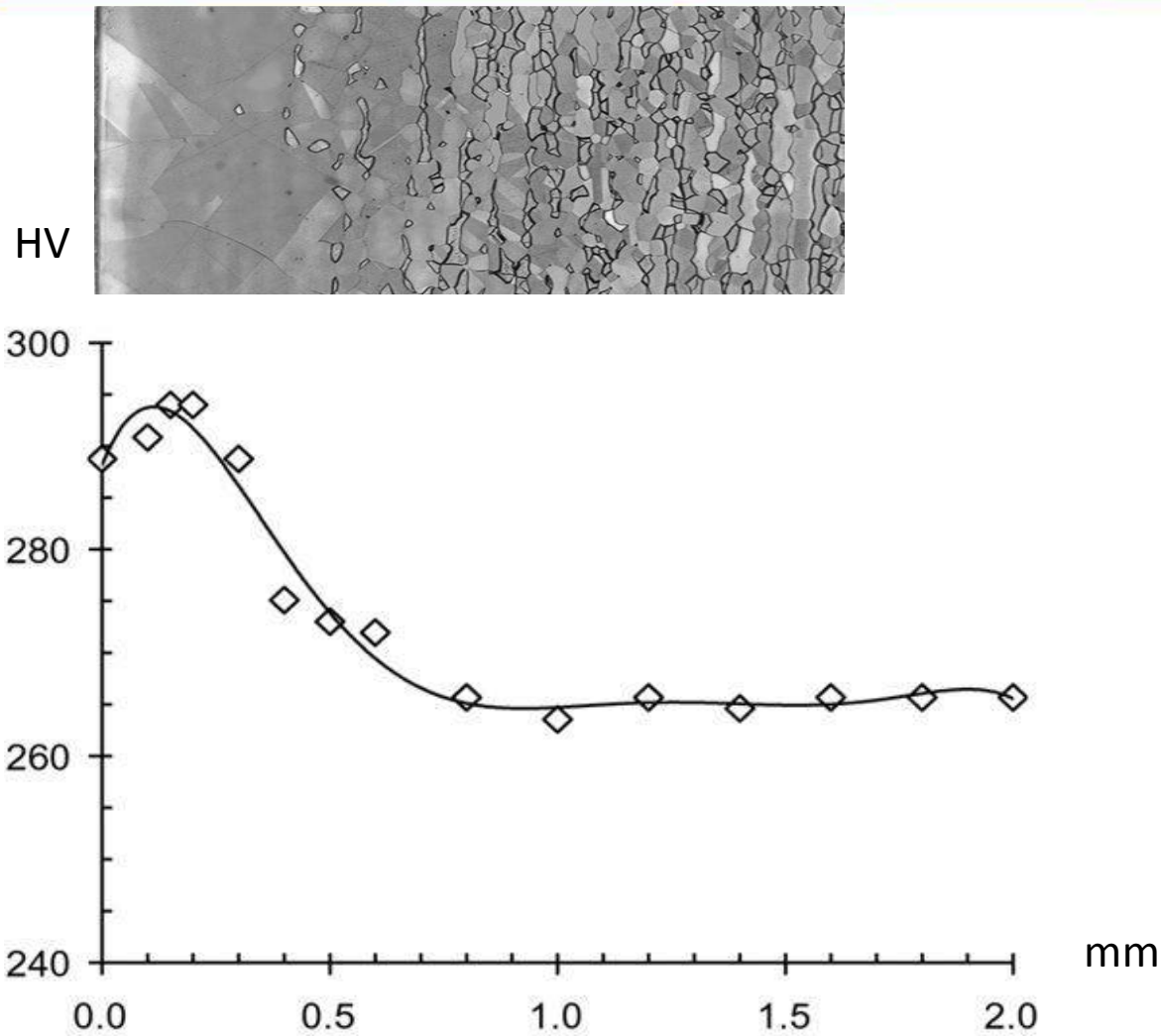


(c) HTGN at 1150 ° C for 3 min



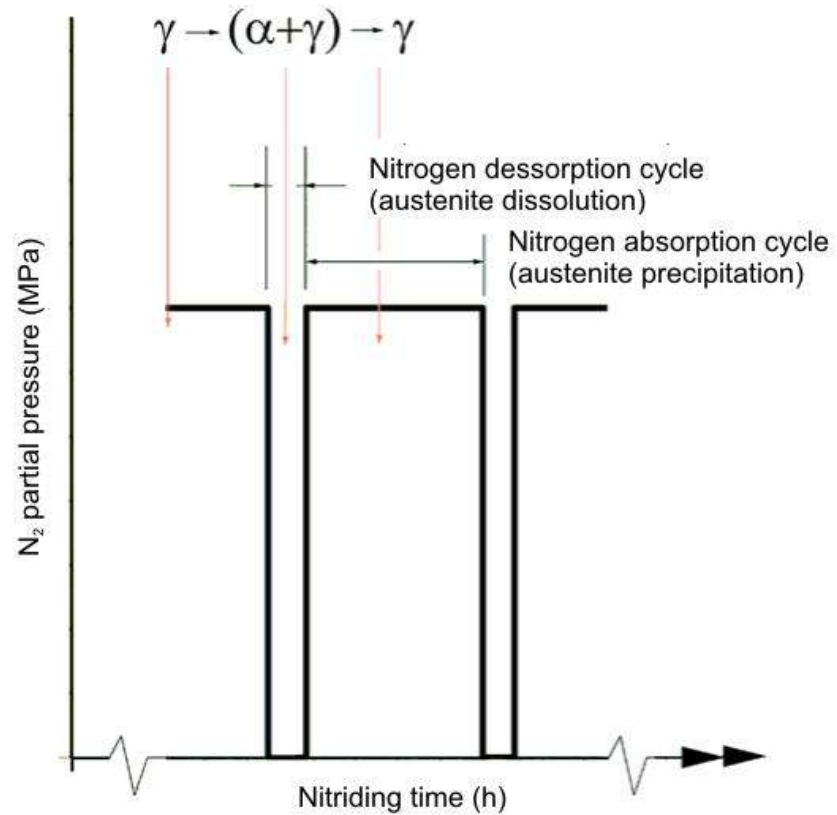
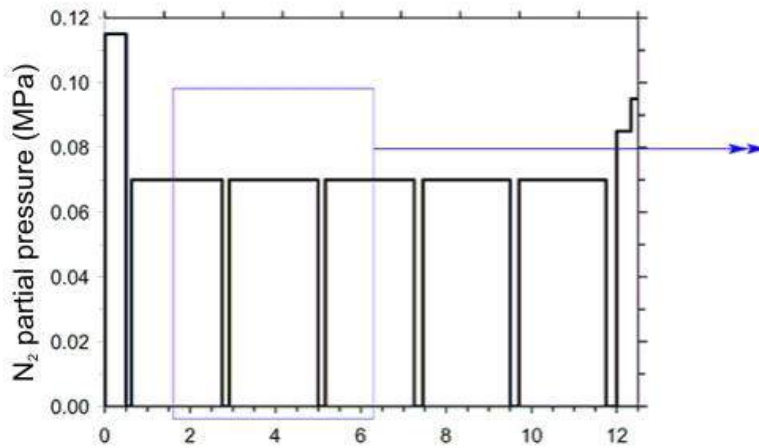
(d) HTGN at 1150 ° C for 45 min

UNS S31803 duplex stainless steel during HTGN treatment at 1150°C

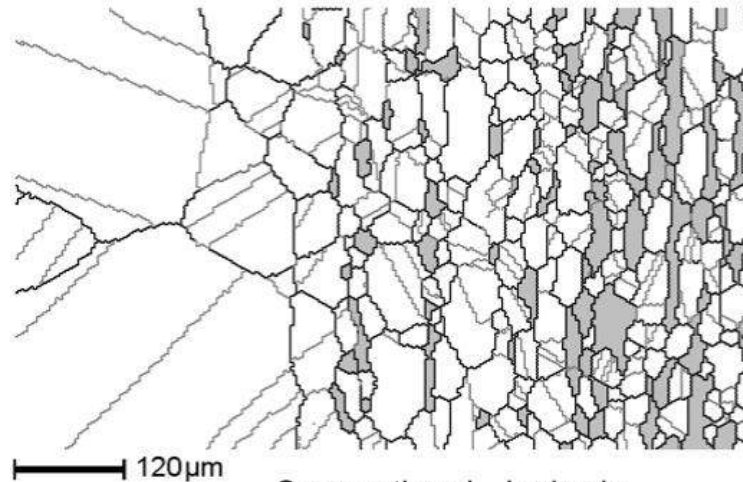


Hardness of UNS S31803 DSS after HTGN treatment at 1150°C

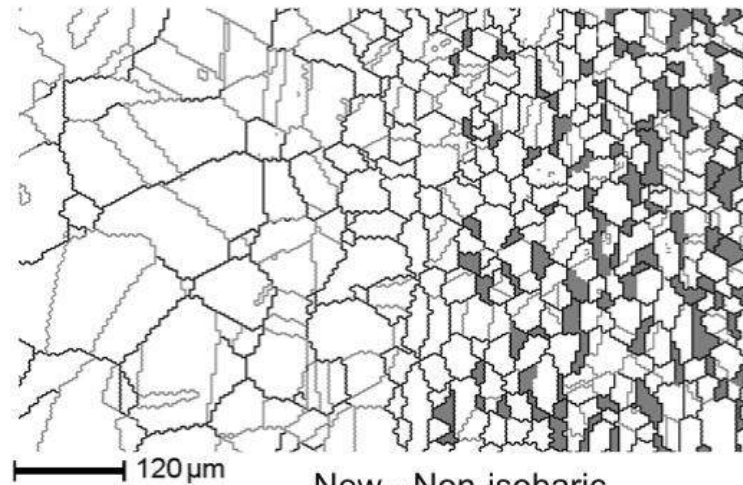
Non isobaric treatment for grain refinement



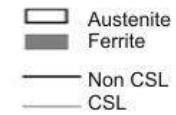
Non isobaric treatment for grain refinement



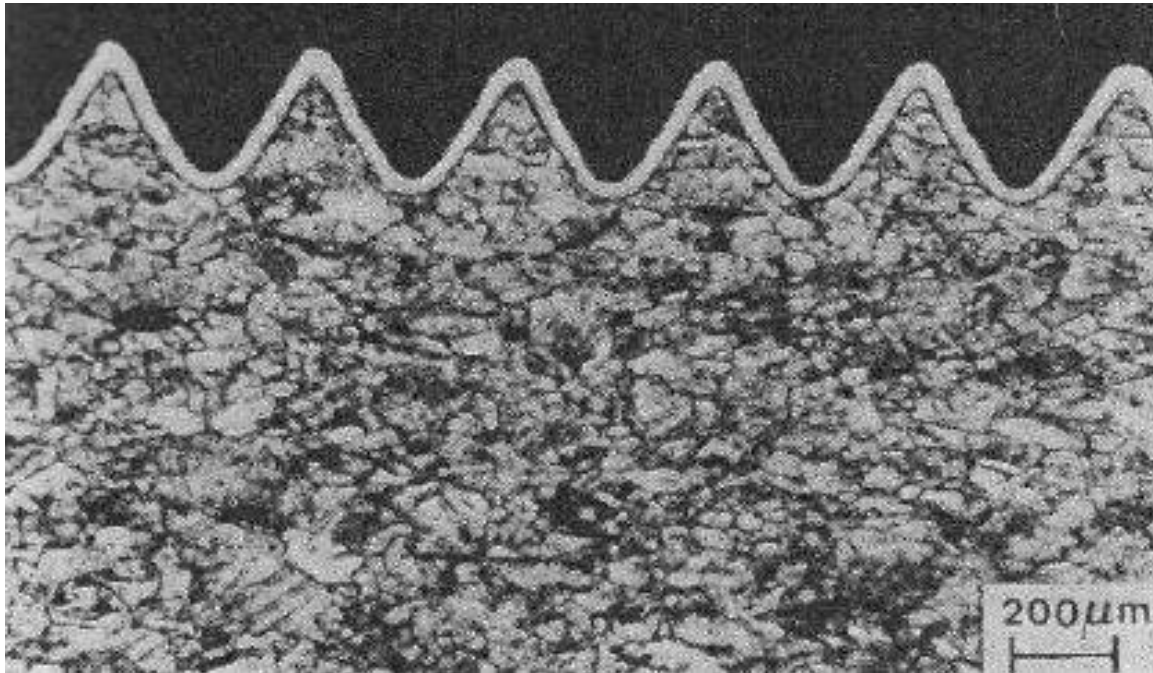
Conventional - Isobaric



New - Non-isobaric

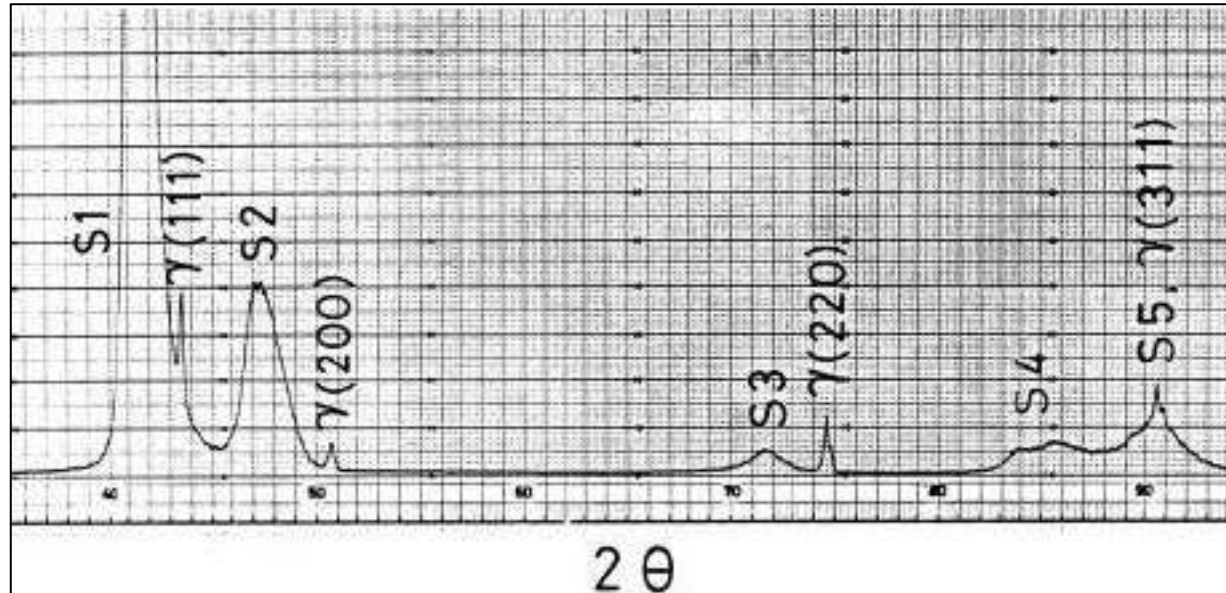


IMPROVEMENT OF SURFACE HARDNESS WITHOUT LOSS OF CORROSION RESISTANCE



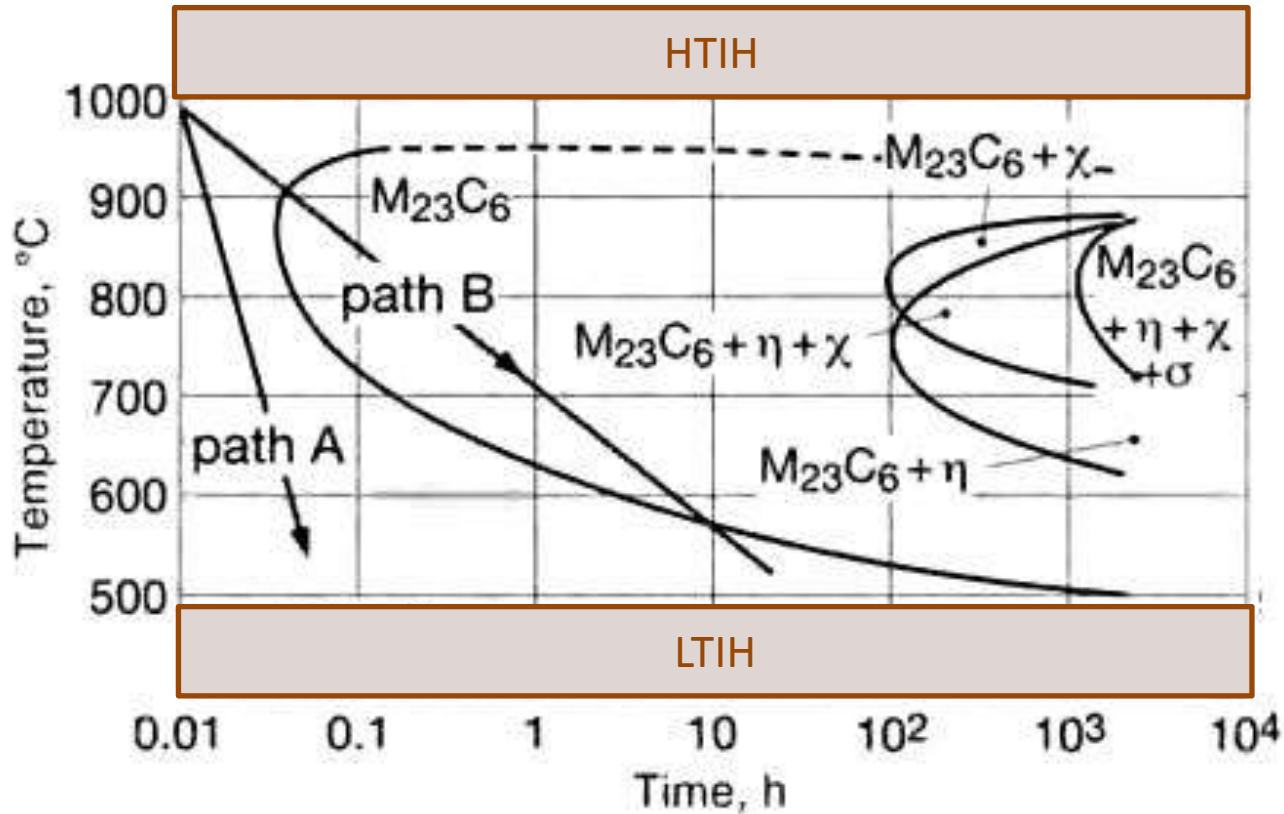
Kolsterising

A “new phase” identified by Ichii et al., the so-called S phase.
Peaks of a cubic phase **shifted (S)** to the left.



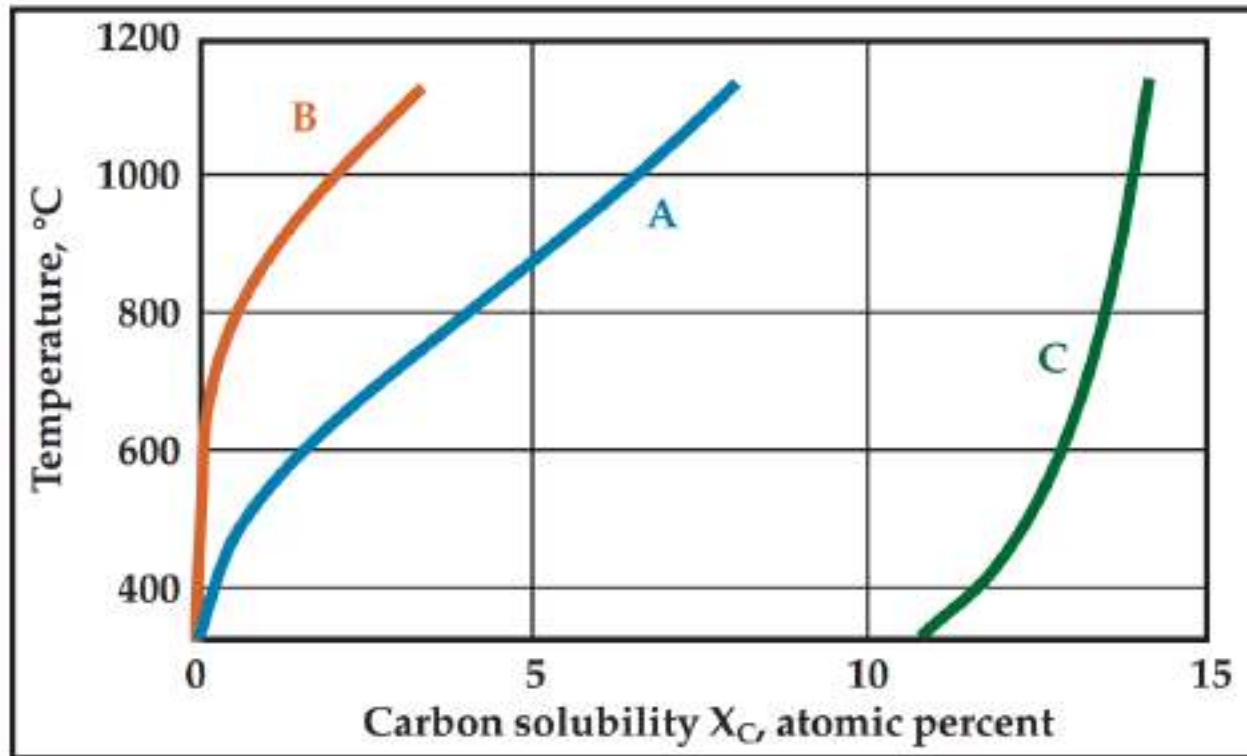
- ✓ metastable,
- ✓ precipitate free,
- ✓ interstitial supersaturated,
- ✓ superhard ‘expanded austenite’,
- ✓ form at low temperatures
- ✓ introduction of interstitials (such as N and C, or both) into an FCC structured substrate

Improve surface hardness without loss of corrosion resistance – Interstitial Hardening



Paths A and C avoid Cr₂₃C₆ precipitation, that harms the corrosion resistance

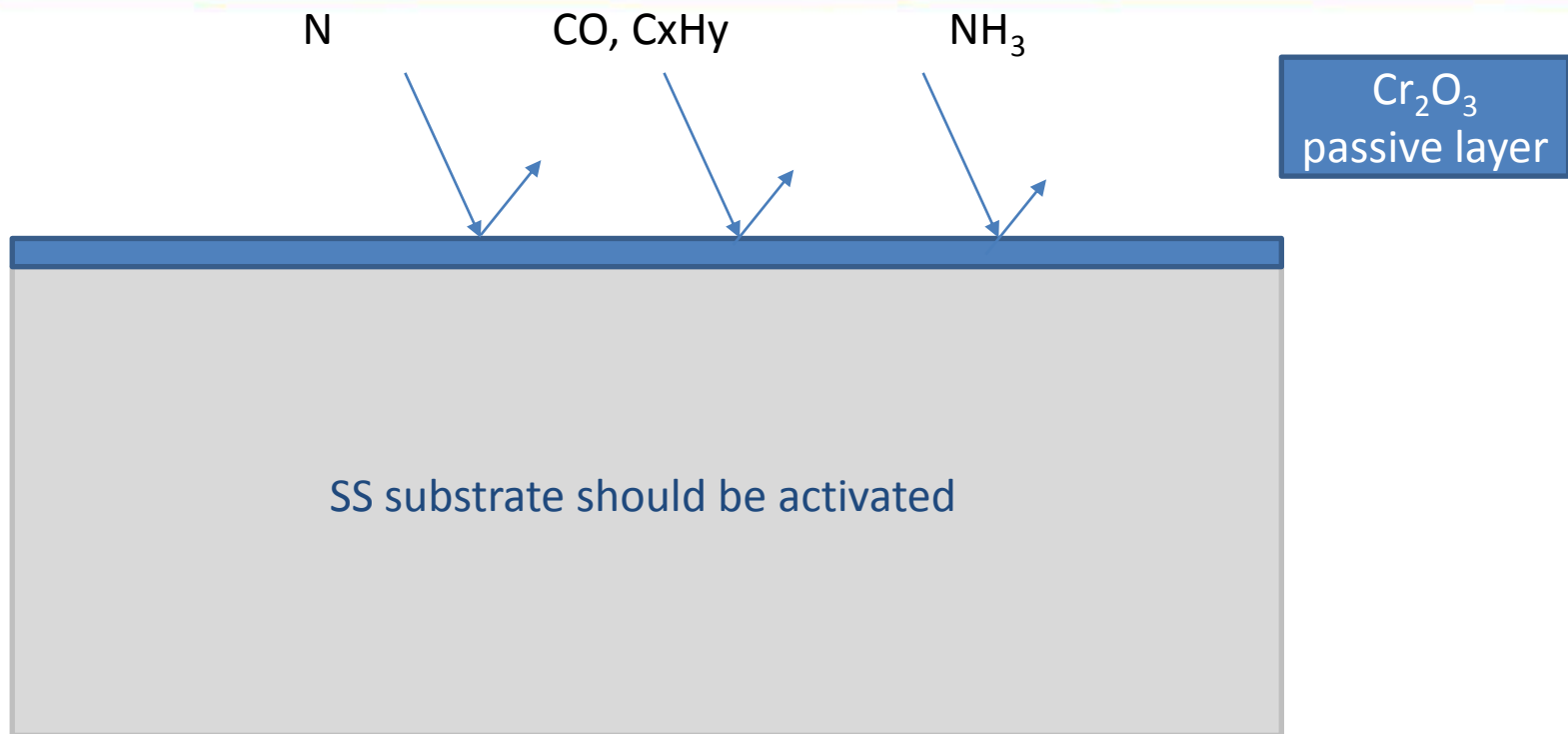
HTIH and LTIH allows hardening without losing corrosion resistance



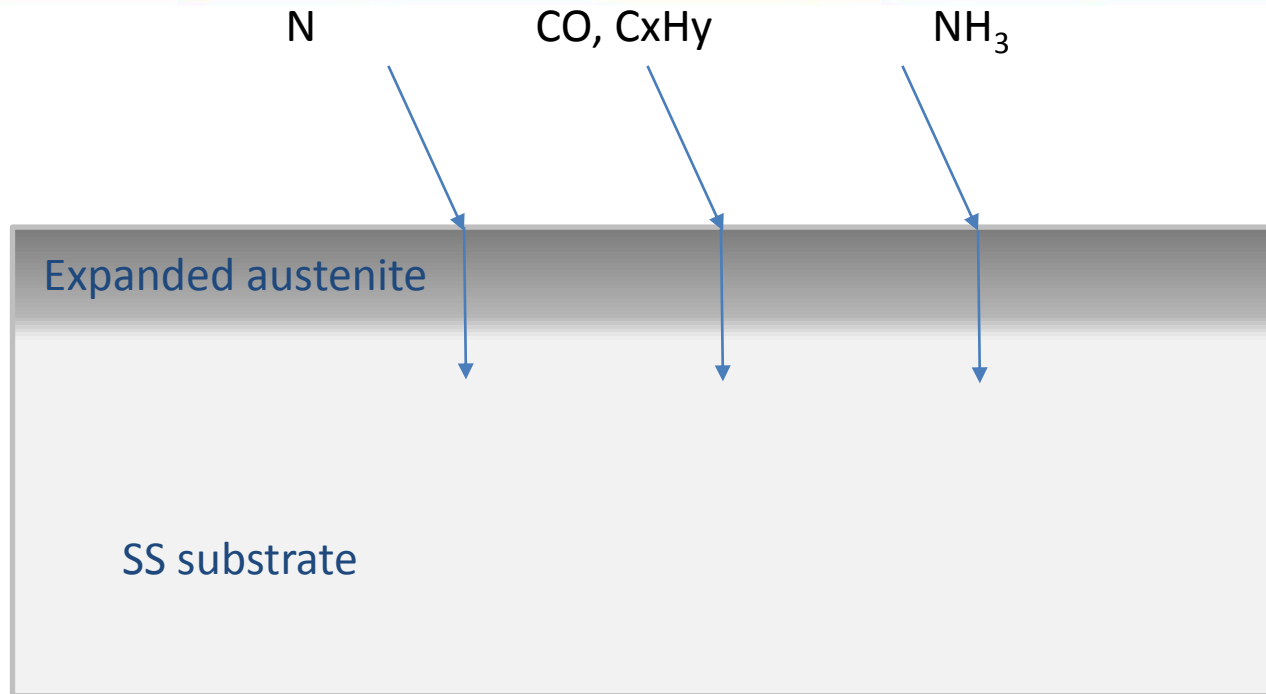
A = Pure iron

B = 316 SS with Cr_7C_3 formation

C = 316 SS without Cr_7C_3 formation

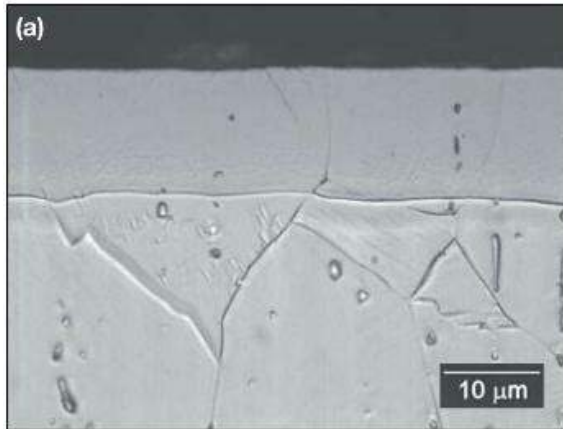


- 1) Depassivation by Halide containing atmospheres: NF_3 or HCl – Low Temperature Gas Carburizing (patent by Swagelok).
- 2) Activation of the surface of the part \Rightarrow Ni metal to prevent repassivation \Rightarrow catalytic NH_3 gas decomposition – (Patent by Somers US 7431778 B2).
- 3) Activation of the surface by sputtering in H_2 , under a high applied voltage and low pressure – Patent 018090023300 INPI – by Tschiptschin .

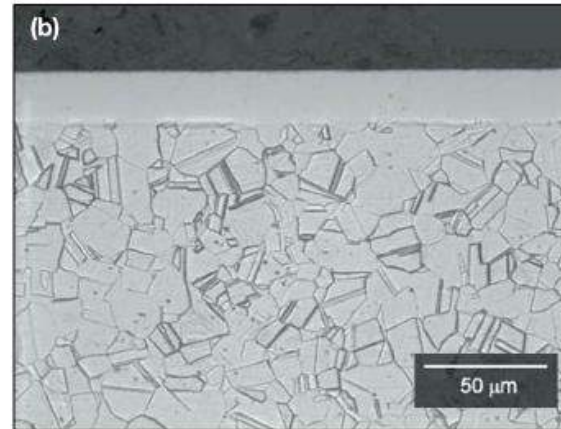


- 1) Depassivation by Halide containing atmospheres: NF_3 or HCl – Low Temperature Gas Carburizing (patent by Swagelok).
- 2) Activation of the surface of the part \Rightarrow Ni metal to prevent repassivation \Rightarrow catalytic NH_3 gas decomposition – (Patent by Somers US 7431778 B2).
- 3) Activation of the surface by sputtering in H_2 , under applied voltage and low pressure – (Patent 018090023300 INPI – by Tschiptschin).

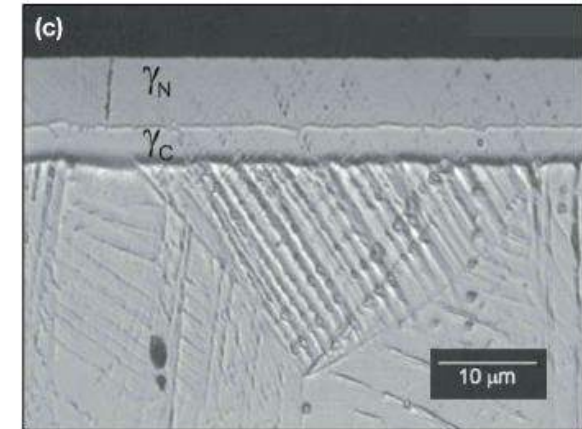
LTPN



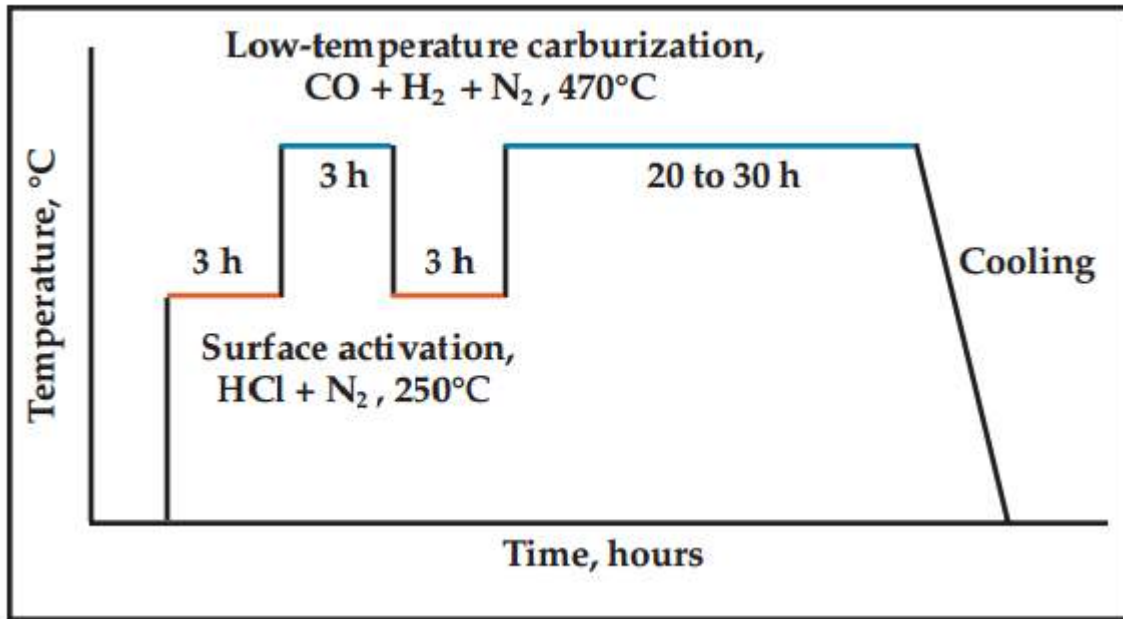
LTGC



LTGNC



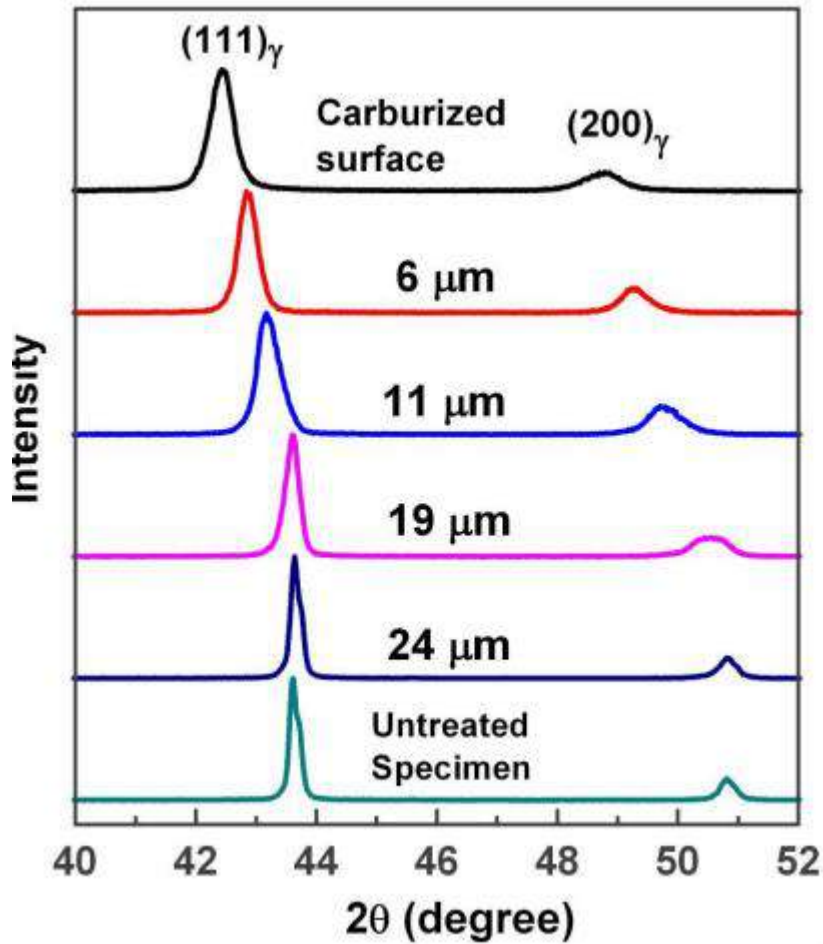
- ✓ metastable,
- ✓ precipitate free,
- ✓ interstitial supersaturated,
- ✓ superhard 'expanded austenite',
- ✓ form at low temperatures
- ✓ Introduction of interstitials (such as N and C, or both) into an FCC structured substrate



Swagelok

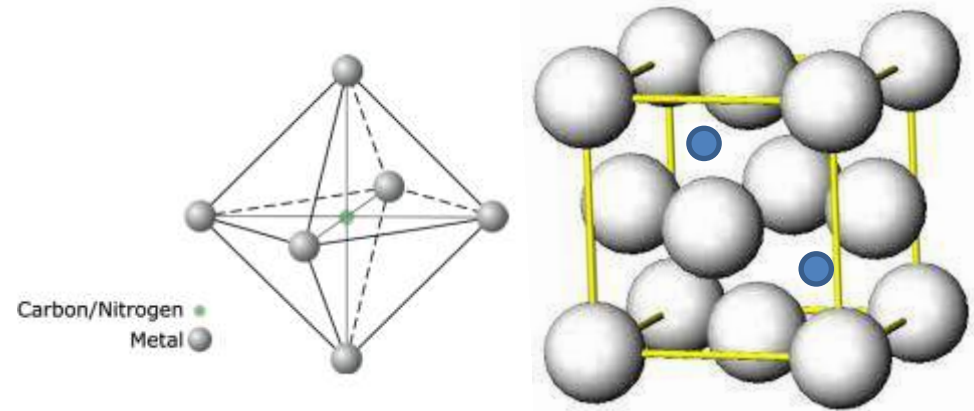


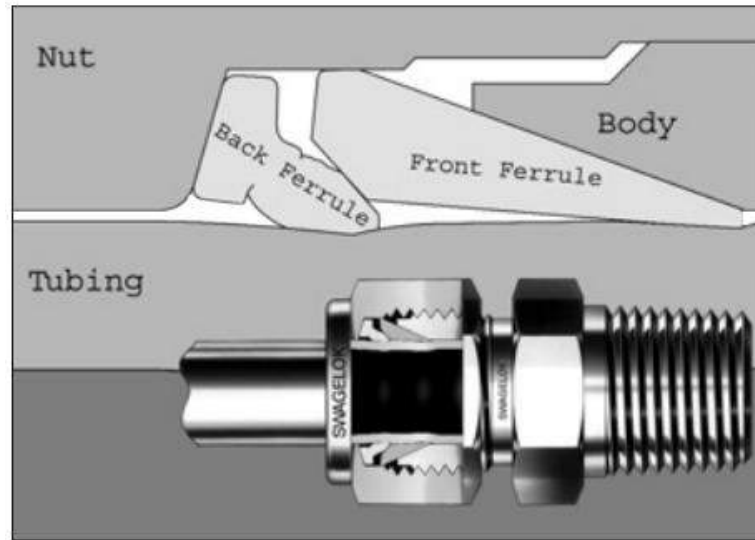
C Expanded Austenite



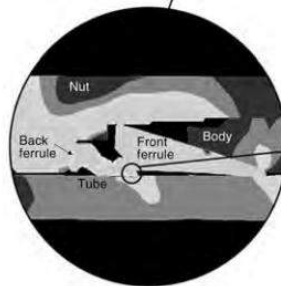
$$a_{\gamma} = a_0 + a \alpha X_C$$

$$\alpha = 0.00104 \text{ nm / at\%}$$



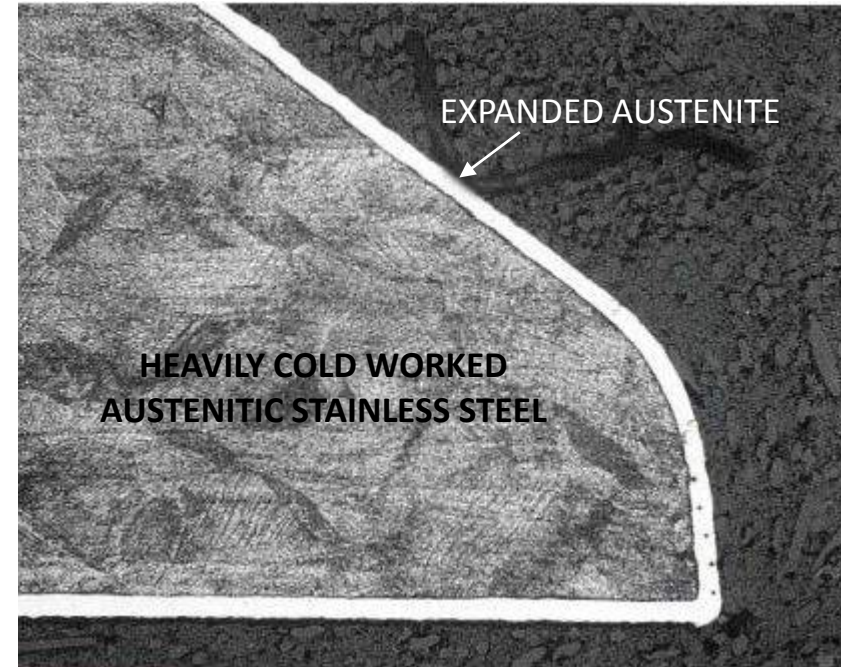
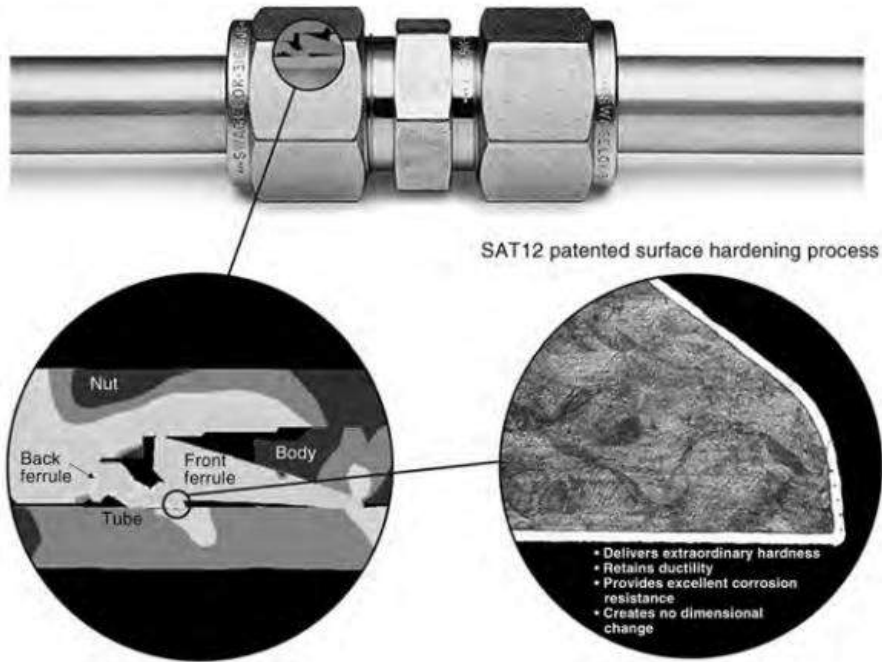


SAT12 patented surface hardening process



- Delivers extraordinary hardness
- Retains ductility
- Provides excellent corrosion resistance
- Creates no dimensional change

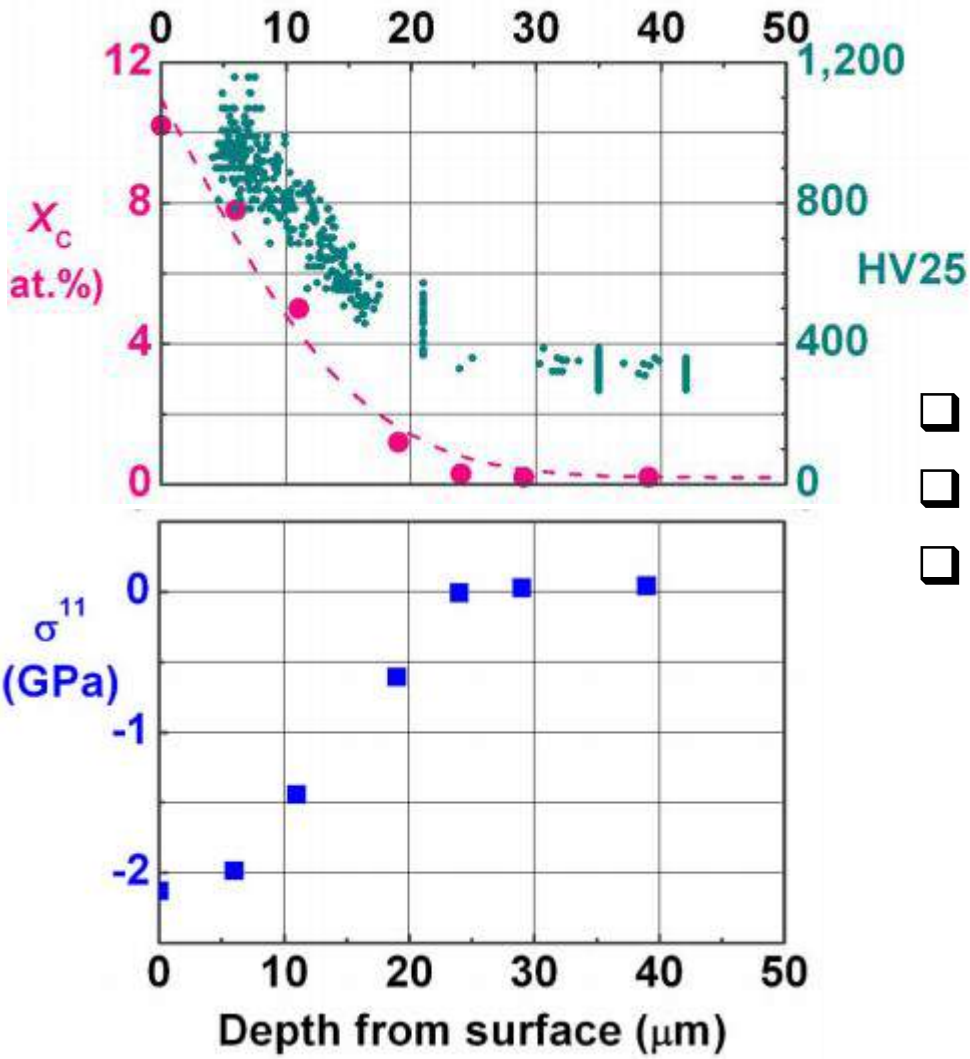
Stainless Steel Fittings



Swagelok development:

- The hardened back-ferrule drives onto the surface of super duplex tubing
- Pressure enough to ensure predictable, leak tight installation and performance at working.

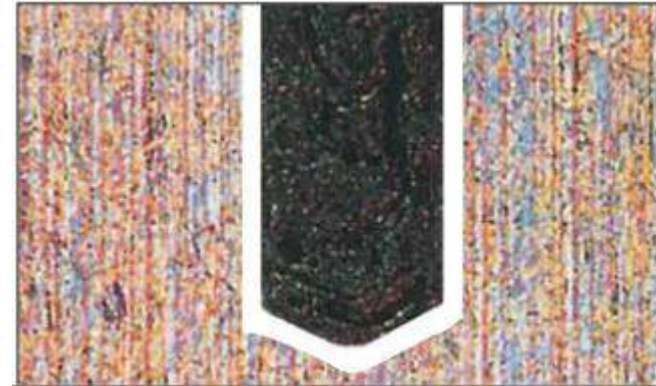
C Expanded Austenite

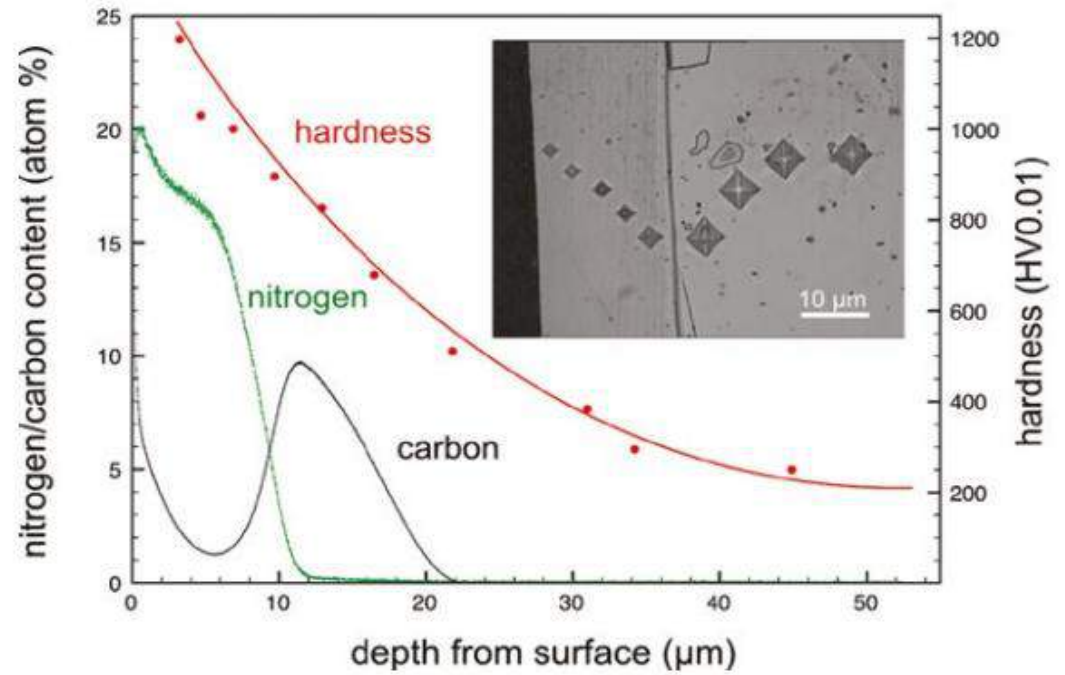
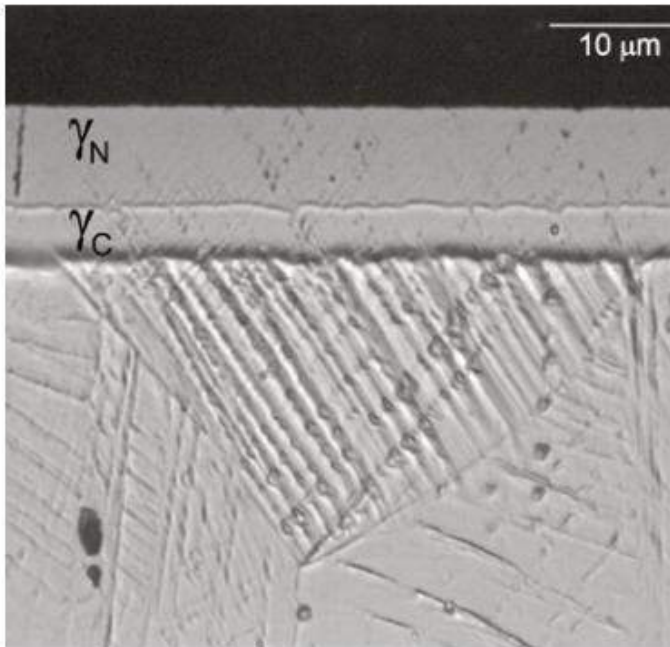


- Hardening depth ~30 μm
- Maximum hardness ~900 HV
- Compressive residual stresses 2 GPa

Bodycote

Kolsterising®

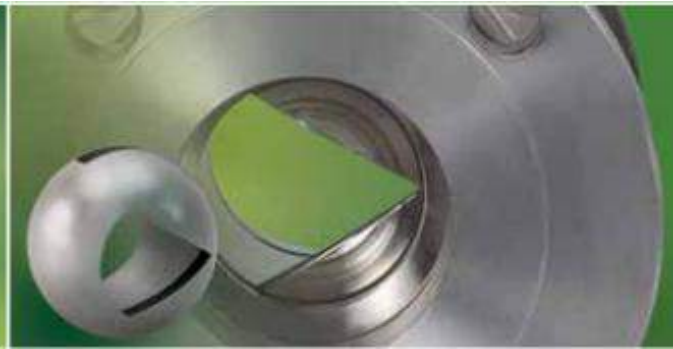






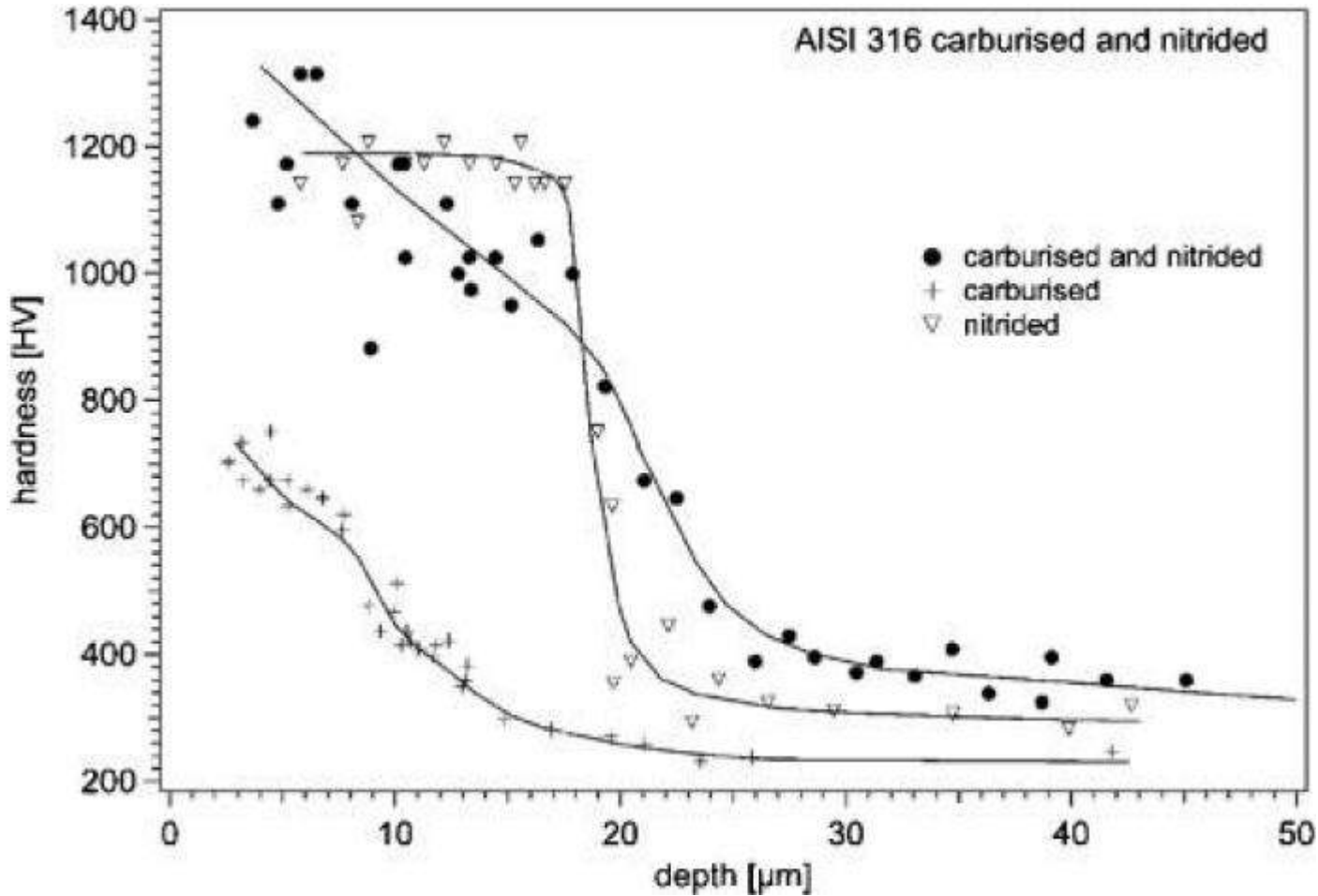
Surface hardening of stainless steel





- ❑ Surface hardening of stainless steel ball valves

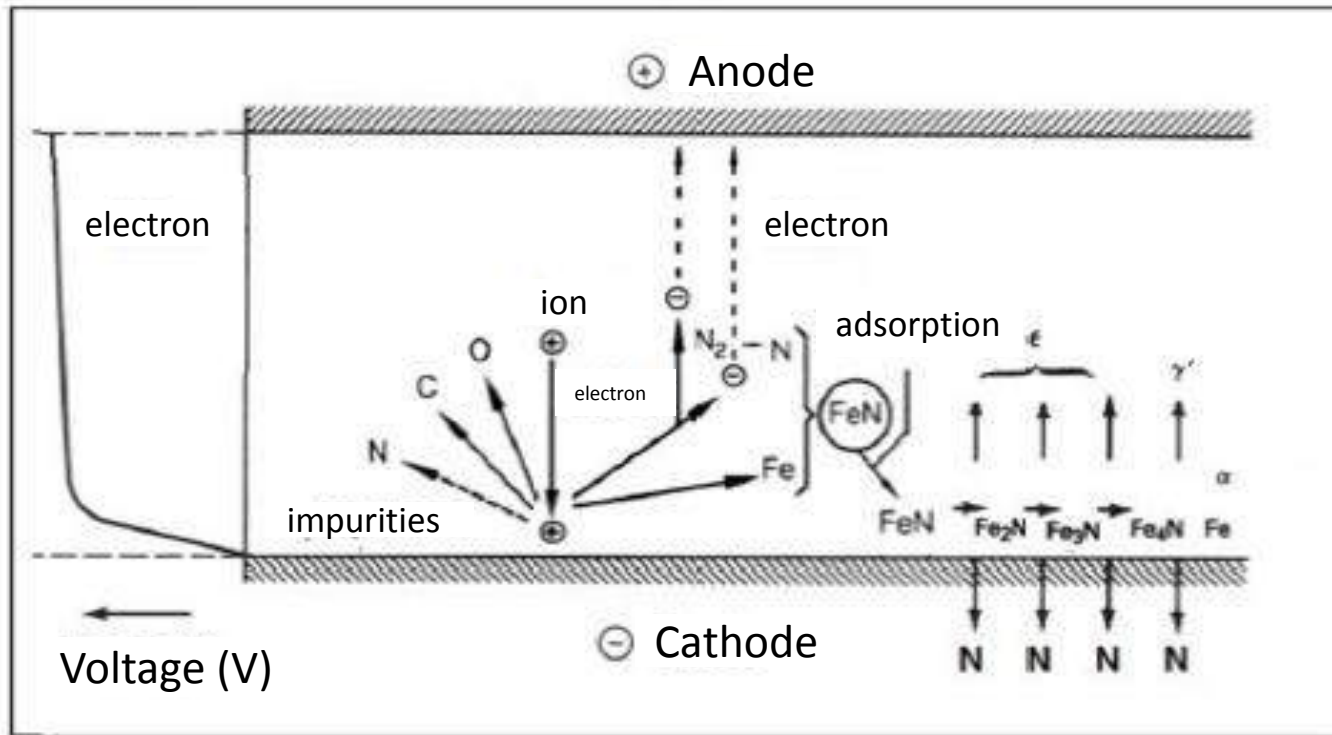
Properties	(γ_N)	(γ_C)
Formation temperature, °C	300–450	400–550
Surface interstitial content, at.-%	20–30 (<30)	5–10 (<15)
S-phase layer thickness, μm	10–20 (<30)	20–40 (<50)
Surface hardness, HV0.05	1300–1500	800–1000
Hardness depth distribution	Abrupt change	Gradual change
Load bearing capacity	Low	High
Ductility/toughness	Poor	Good
Residual stresses	High but shallow	Low but deep
Fatigue properties	Low	High
Pitting corrosion resistance	Very good	Good
Dry sliding wear resistance	Very good	Good
Corrosion wear in saline solution	Very good	Good
Fretting wear in Ringer's solution	Very good	Good
Erosion corrosion in silica/saline slurry	Very good	Good
Thermal stability	Low	High
Biocompatibility	Good	Good



- N expanded austenite - hardening depth ~30 µm
- Maximum hardness ~1200 HV

- Depassivation by H₂ sputtering
 - Ionization of gas molecules and atoms
 - Acceleration of ions towards the cathode
 - Generation and recombination of chemical compounds or radicals , in particular Fe/N ions
 - Condensation of FeN molecules in the cathode surface with release of nitrogen to the surface
 - Penetration of ions in the surface of the part
 - Plasma nitriding (H₂+N₂) least affects the surface finish of the product.
 - Plasma nitriding has a higher surface hardness and maintains your material's core properties due to the lower processing temperatures associated with plasma nitriding
 - Plasma nitriding is environmentally friendly. Plasma nitriding uses non-toxic precisely controlled gas mixtures.

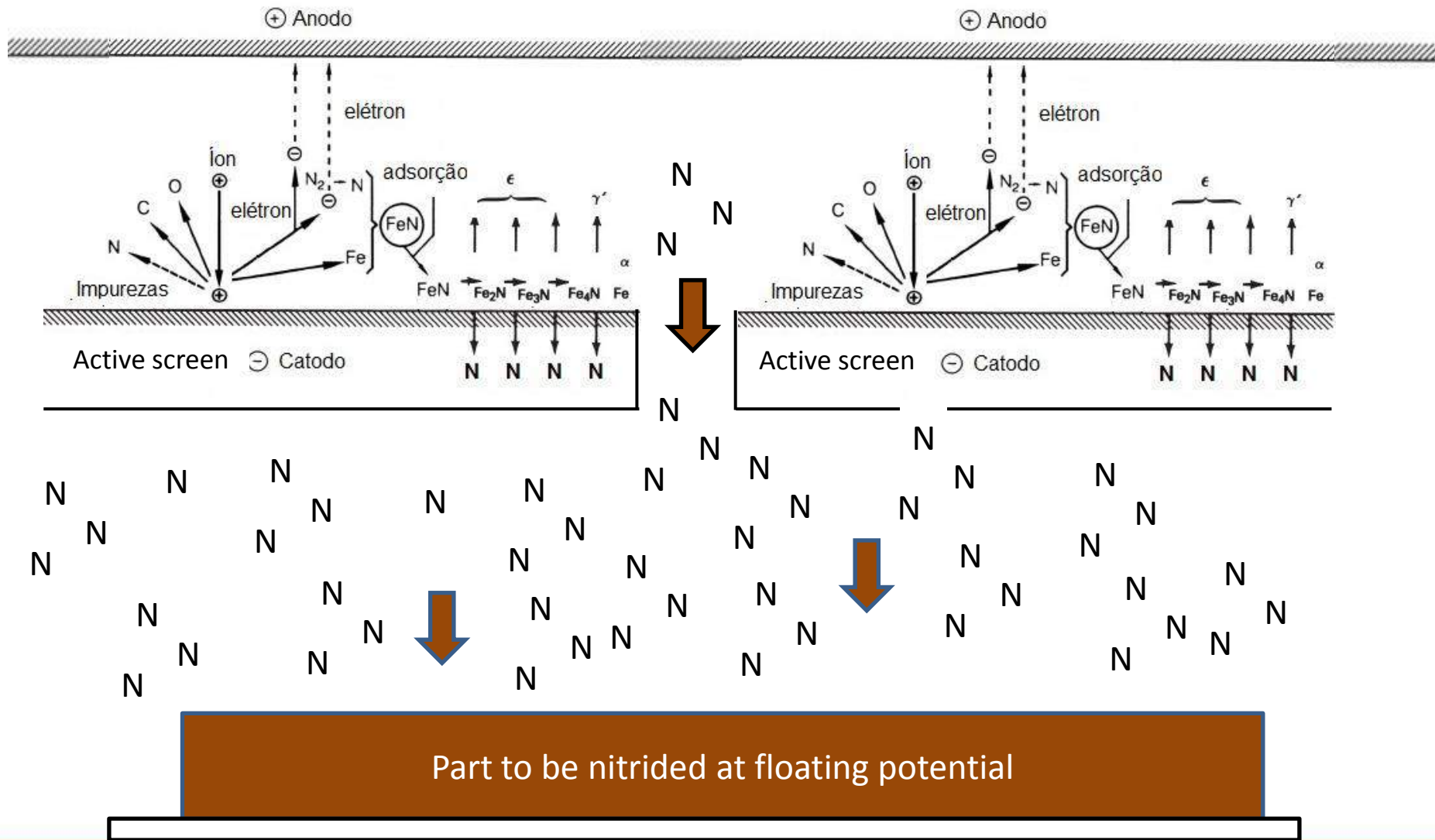
Kölbel Mechanism of Plasma Nitriding



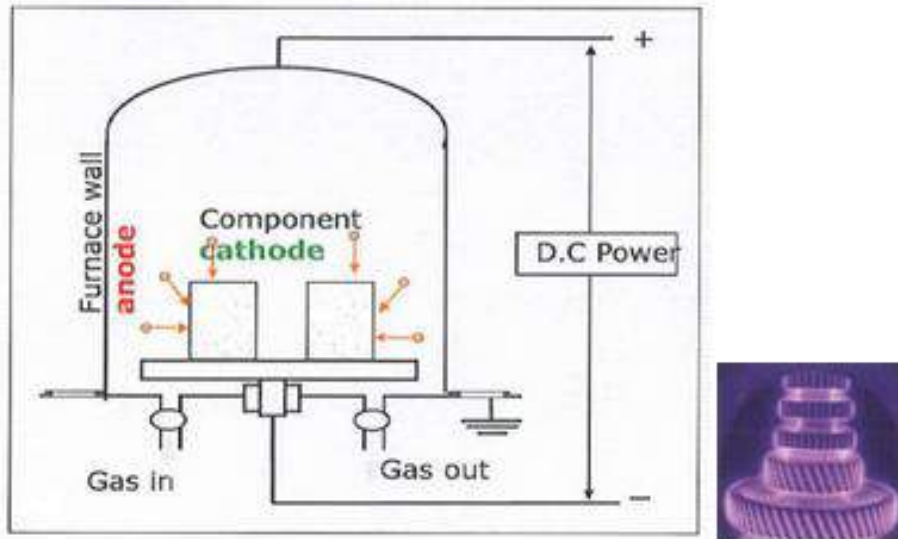
- Disadvantages
 - Rings of different colors are formed when stainless steel parts are pulsed DC plasma nitrided.
 - Distortions of the electric field around the corners and edges,
 - Shape of plasma sheath, which is connected to the shape of samples, determines the ion flux distribution
 - Affects the uniformity, hardness and surface phases of coating.



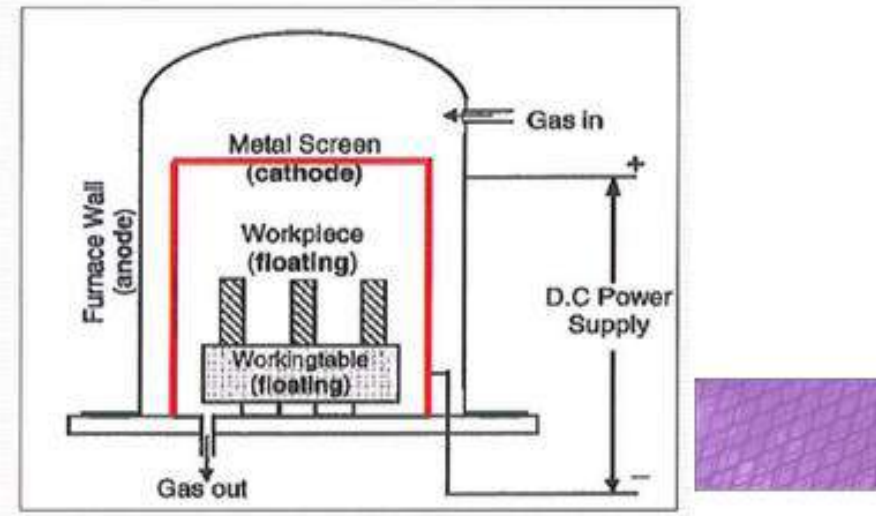
Kölbel Mechanism Operating in Active Screen



- Plasma nitriding reactions occur directly on the surface of the part
- Plasma nitriding reactions occur on the surface of the screen



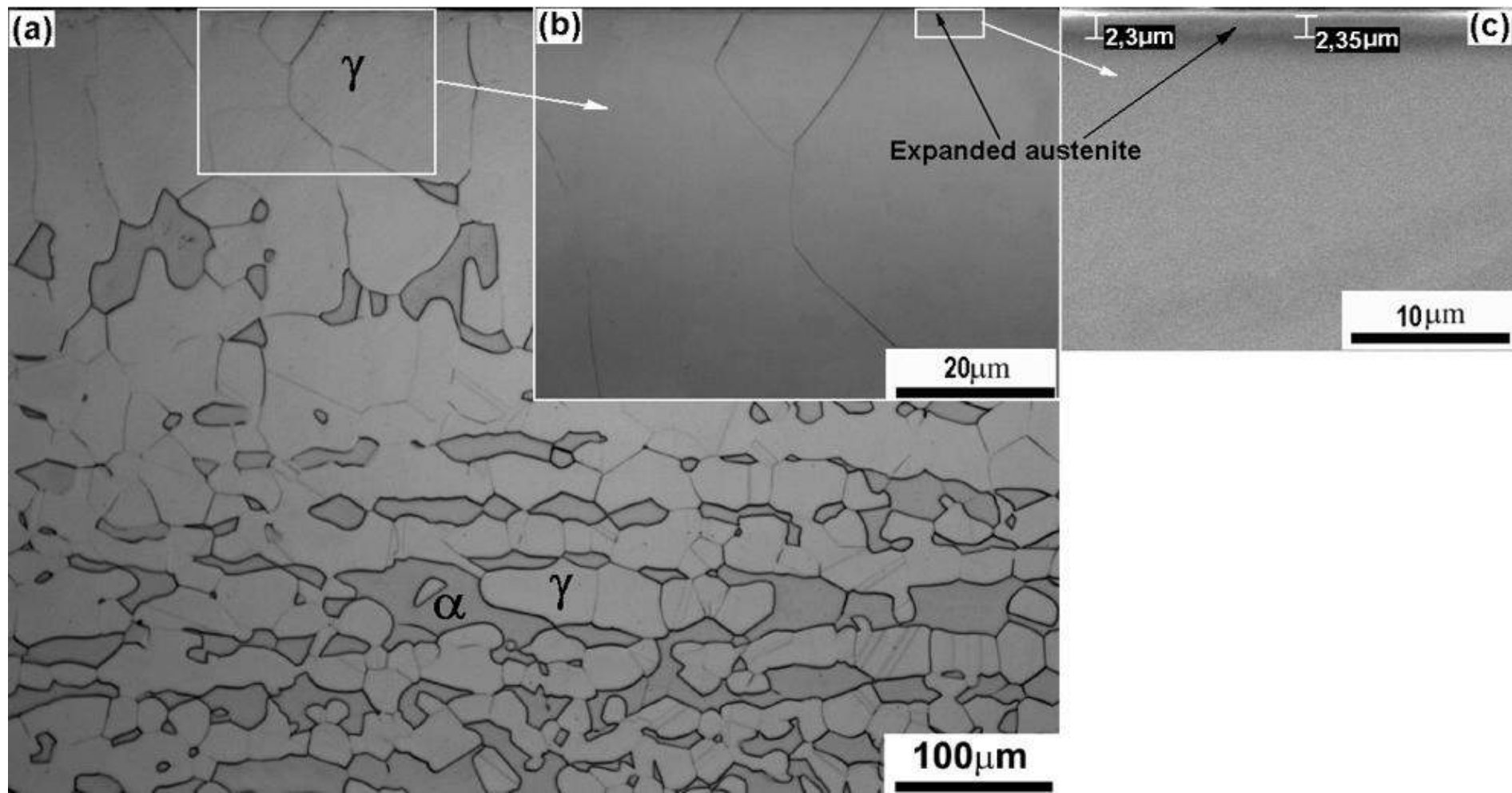
Direct Current Plasma Nitriding



Active Screen Plasma Nitriding

- Higher N potential
- Influence of the part geometry on the nitrogen potential and nitrogen flux
- Edge effect
- Lower N potential
- More homogeneous nitrogen flux throughout the surface
- More even nitrided layer

Duplex Treatment (HTGN + LTPN)

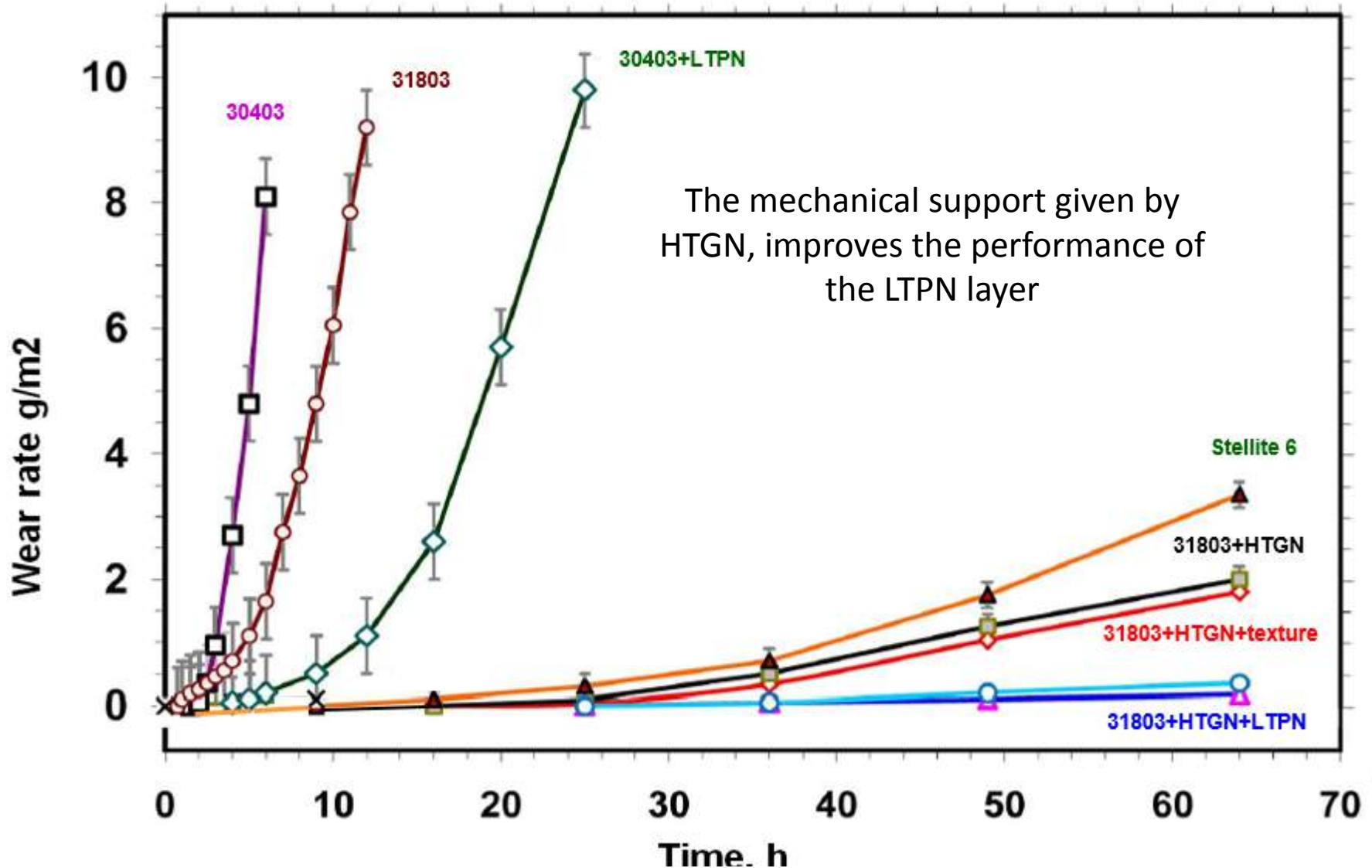


(a) HTGN of duplex stainless steel

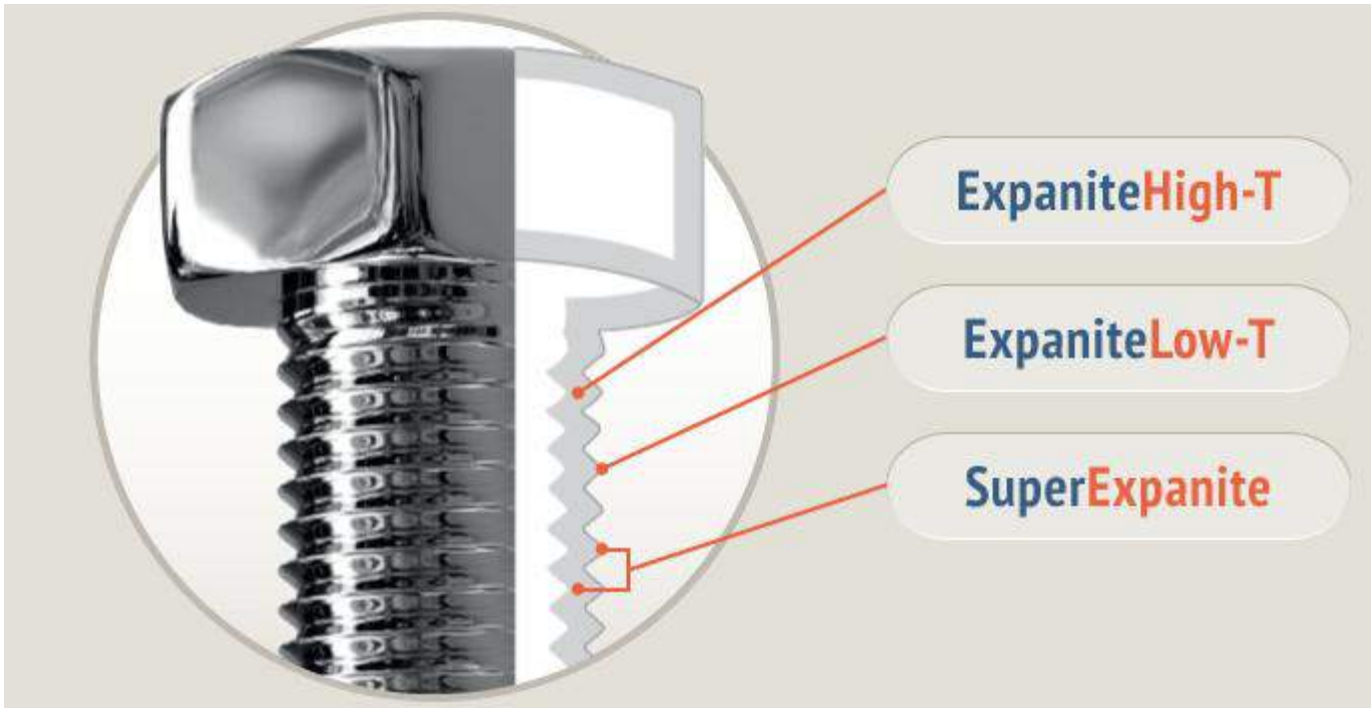
(b) High Nitrogen layer

(c) Expanded austenite layer

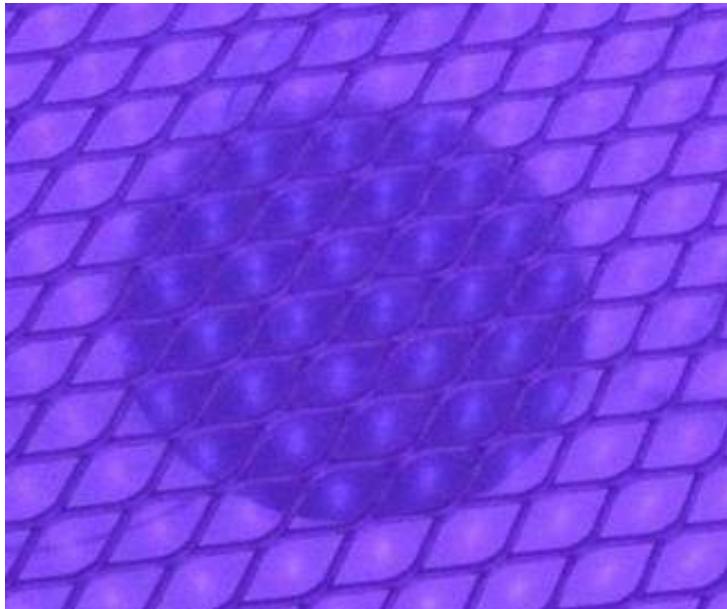
Cavitation Erosion Resistance of Duplex Treated UNS S31803



N Expanded Austenite



The mechanical support given by HTGN, improves the performance of the LTGN layer

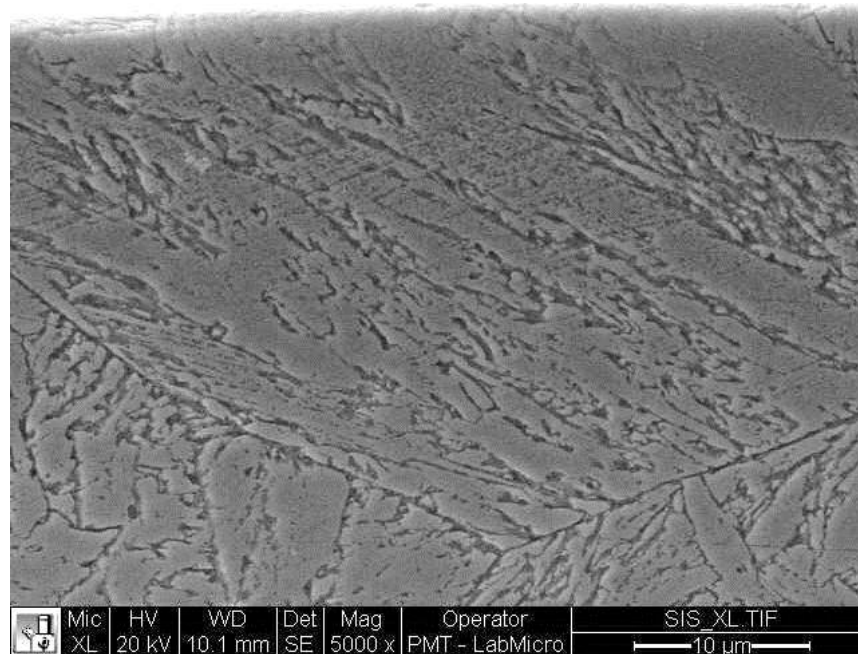


Plasma removed from the parts' surface

Plasma nitriding reactions occur on the surface of the screen

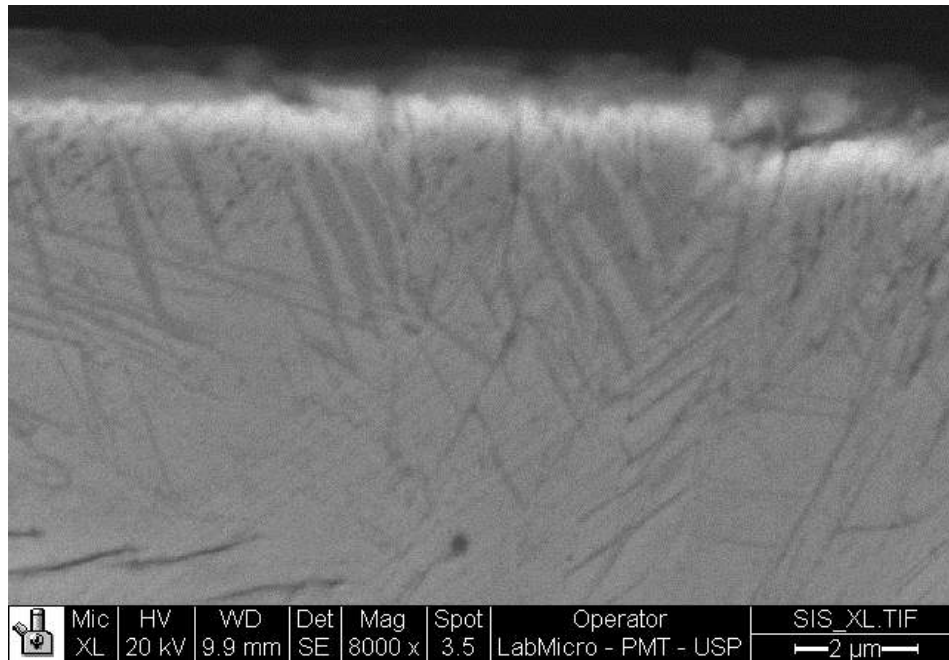


- Martensitic stainless steels are used for manufacturing hydraulic components affected by cavitation erosion.
- The introduction of nitrogen atoms using thermochemical treatments has been proved to be an effective way to enhance the cavitation erosion resistance
- Low temperature nitriding of martensitic stainless steel leads to formation of expanded martensite α'_N , (BCC expanded phase)



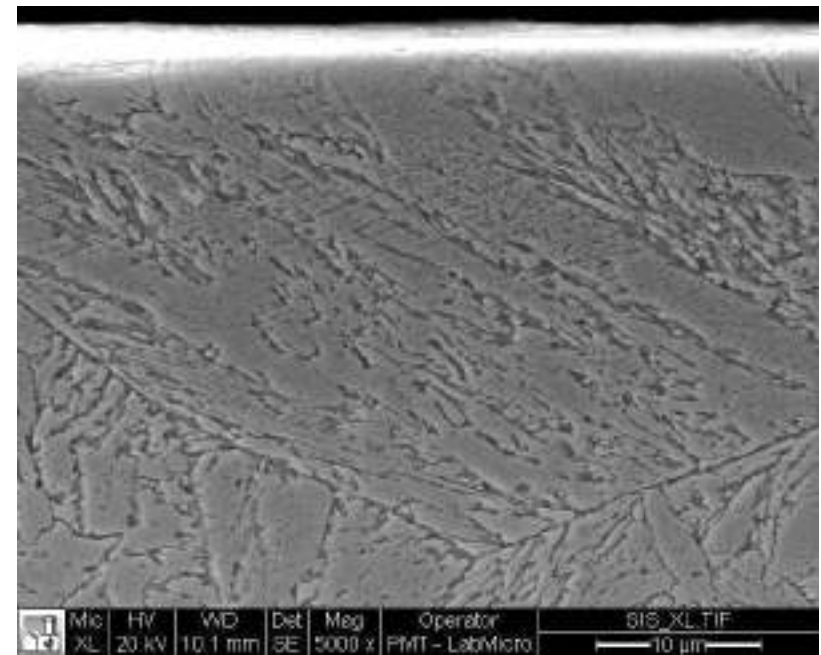
BCC expanded martensite α'_N

- Low temperature nitriding of martensitic stainless steel leads to formation of expanded martensite α'_N , (BCC expanded phase).



DC Plasma Nitriding 400°C, 20 h

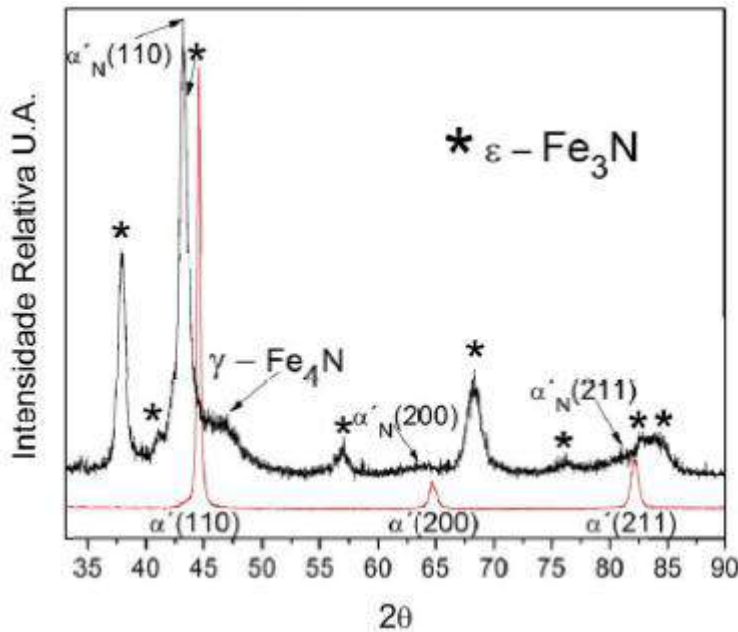
Fe₄N Nitrides + α'_N (BCC expanded phase)



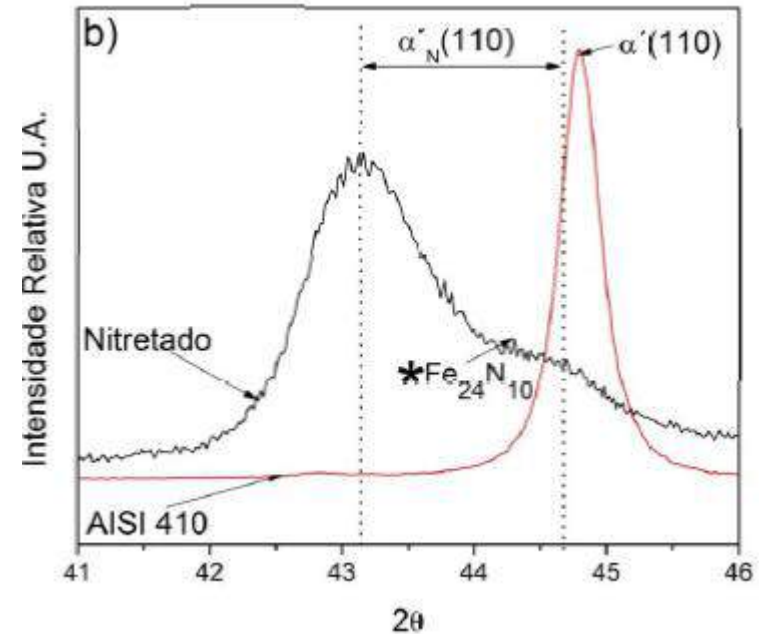
ASPN nitriding 400°C, 20 h

α'_N , (BCC expanded phase).

- Low temperature nitriding of martensitic stainless steel leads to formation of expanded martensite α'_N , (BCC expanded phase).



DC Plasma Nitriding 400°C, 20 h

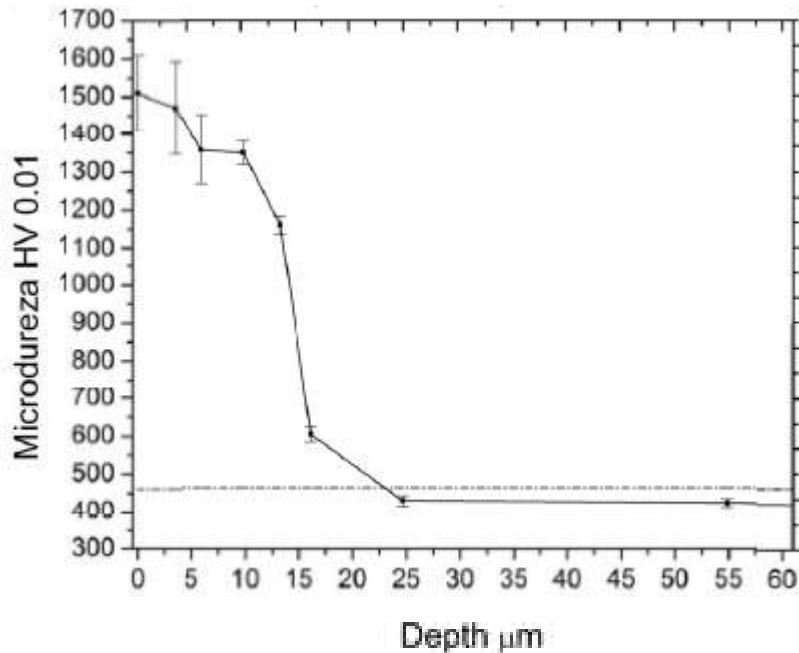


ASPN nitriding 400°C, 20 h

Fe_4N , Fe_3N Nitrides + α'_N (BCC expanded phase)

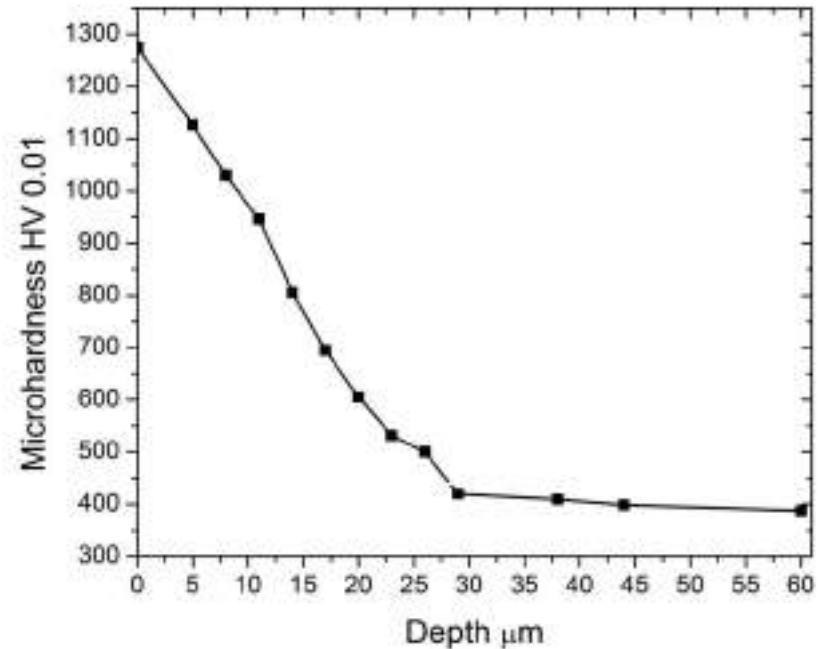
α'_N , (BCC expanded phase).

- Low temperature nitriding of martensitic stainless steel leads to formation of expanded martensite $\alpha'N$, (BCC expanded phase)



DC Plasma Nitriding 400°C, 20 h

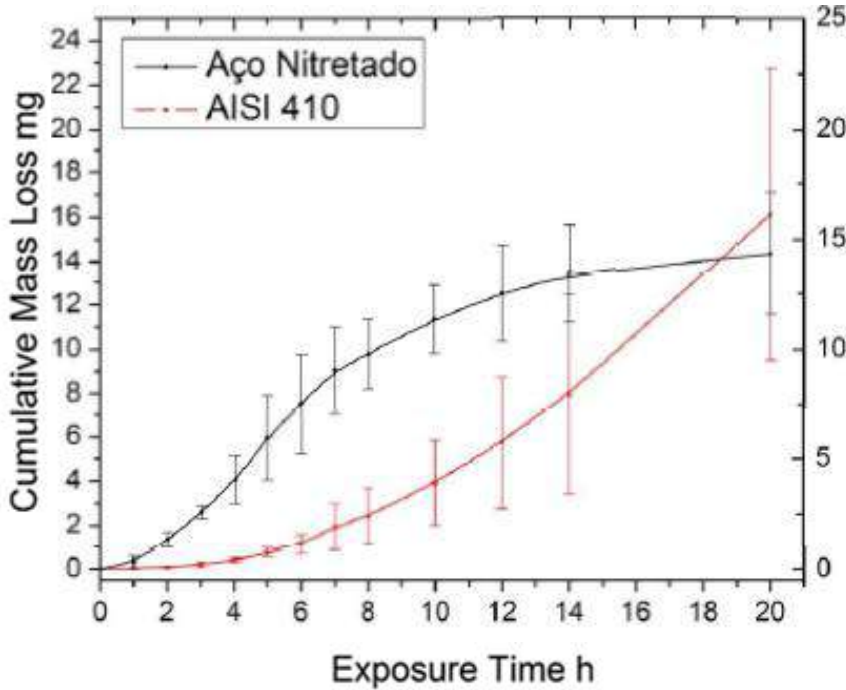
Fe_4N Nitrides + $\alpha'N$ (BCC expanded phase)



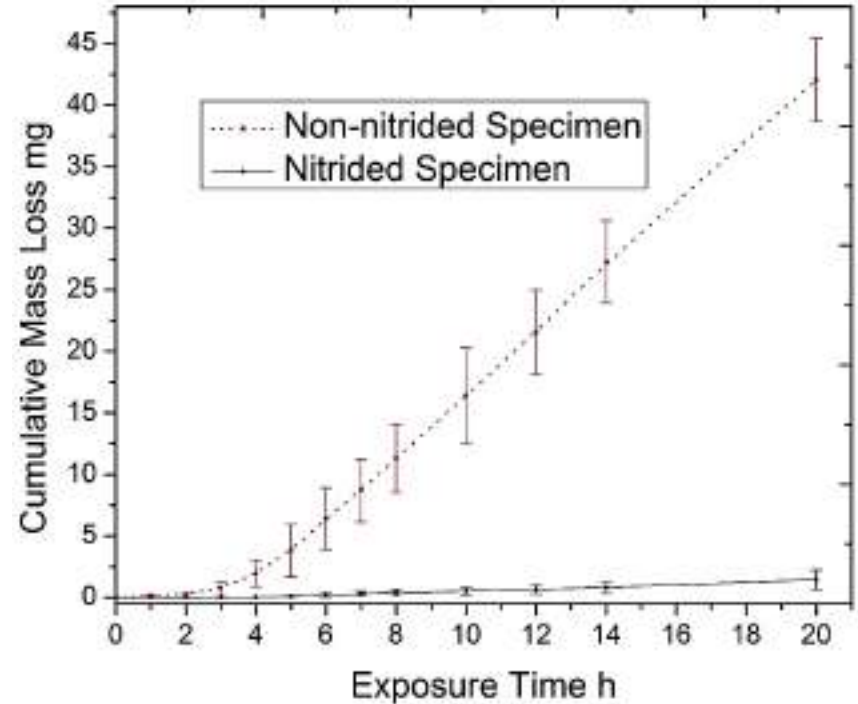
ASPN nitriding 400°C, 20 h

$\alpha'N$, (BCC expanded phase).

- Cavitation erosion resistance



DCPN 400°C, 20 h



ASPN 400°C, 20 h

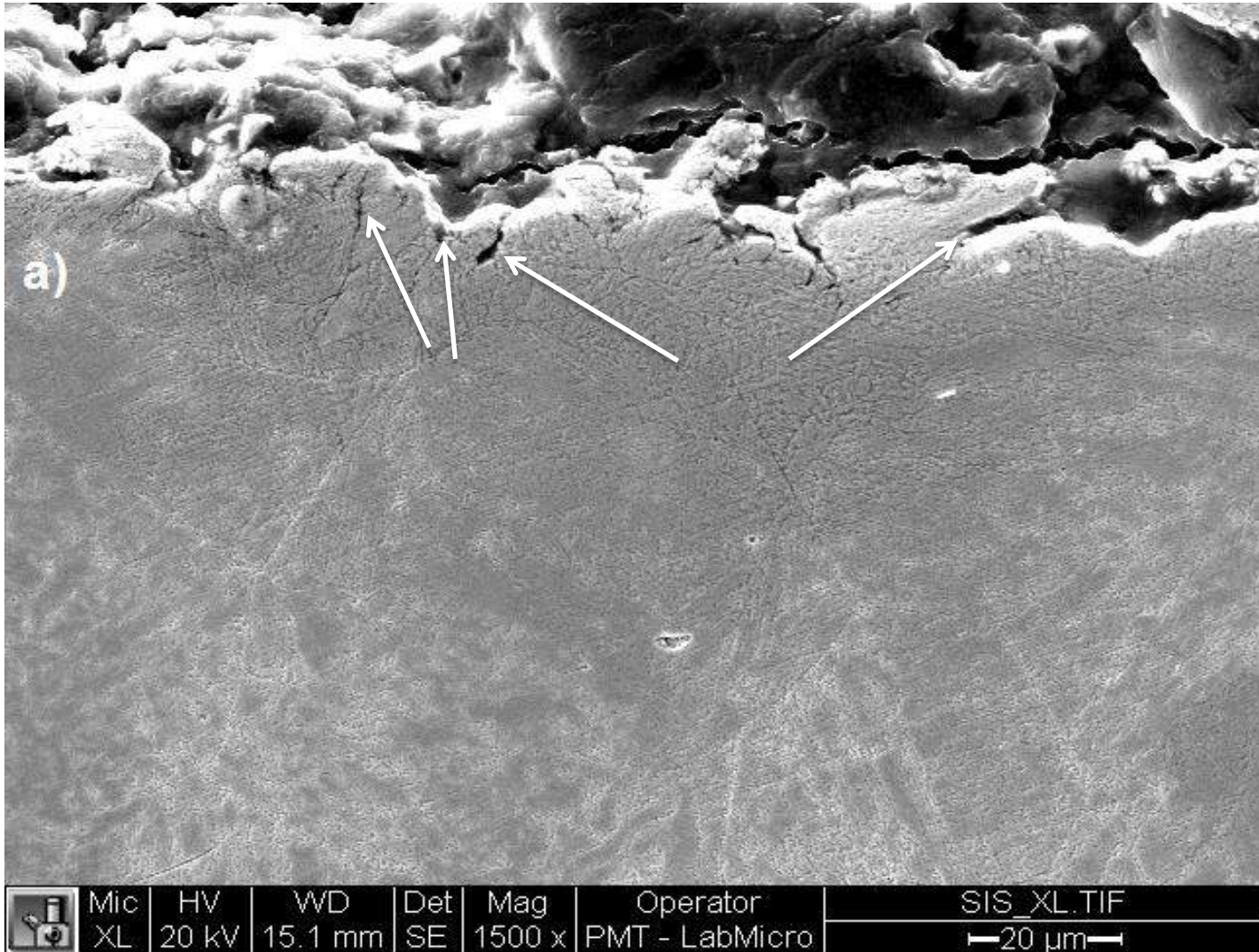
Fe_4N Nitrides + $\alpha'N$ (BCC expanded phase)
 Erosion rates decreased from 1,2 to 0,36 mg/h

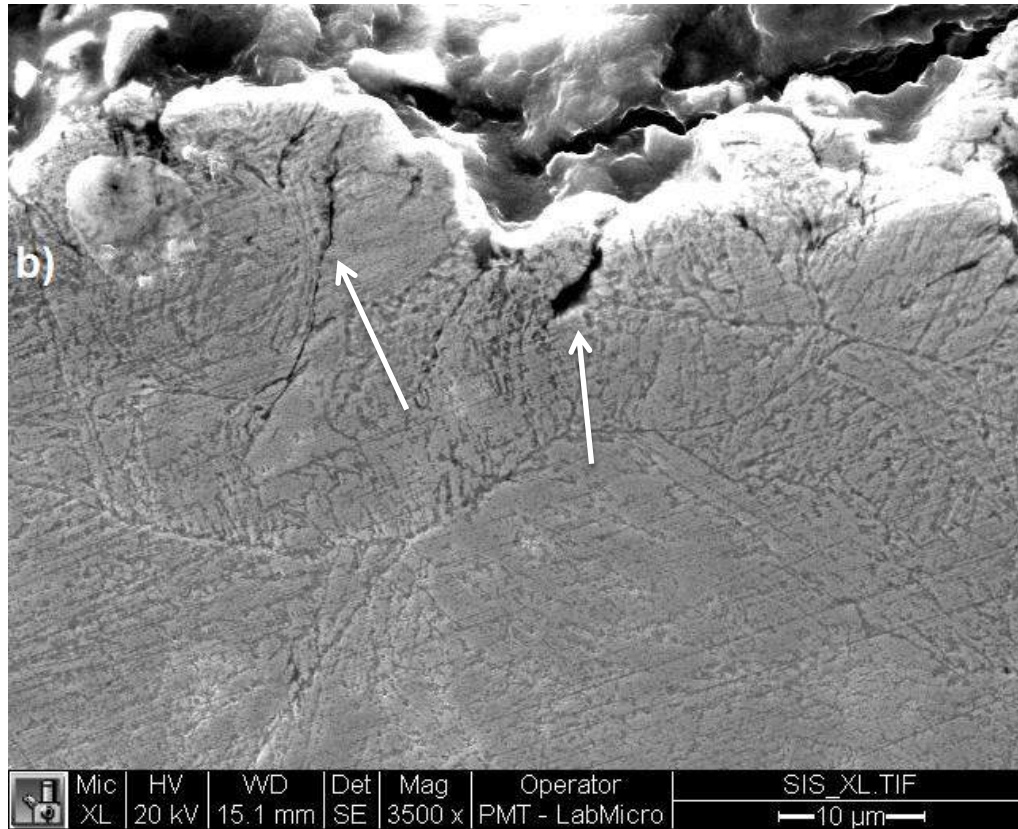
$\alpha'N$, (BCC expanded phase)
 Erosion rates decreased 27 times

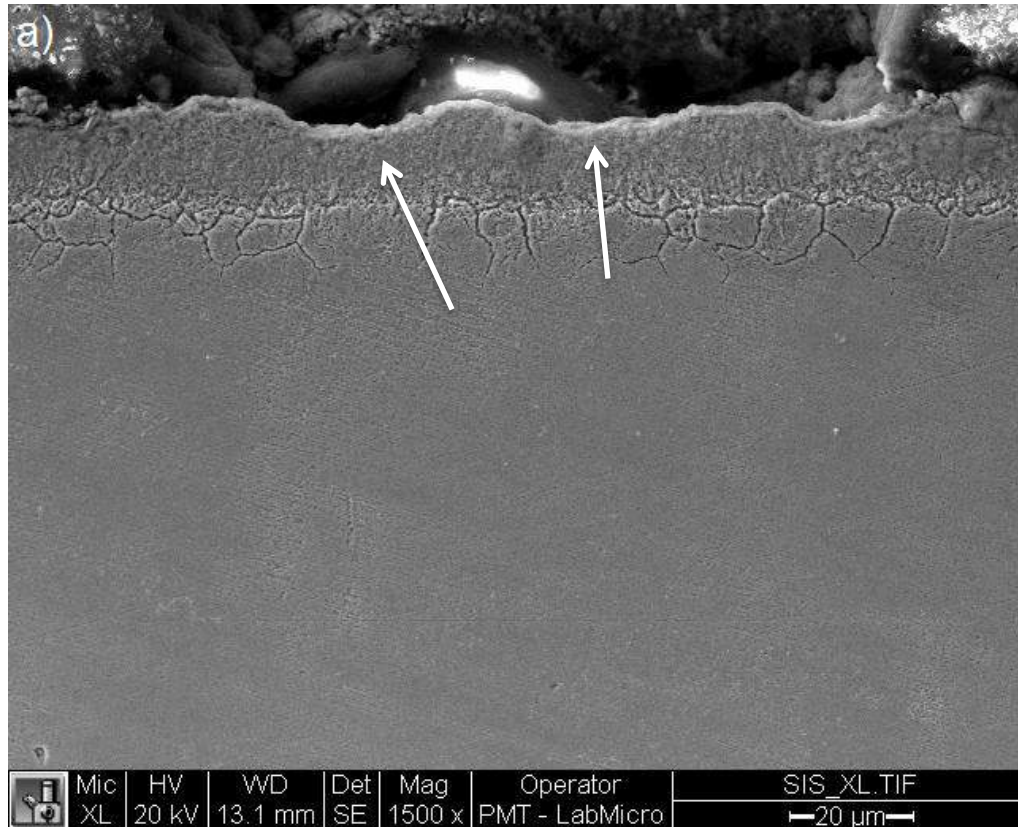
Nanoindentation

Specimen	H (GPa)	h_{max} (nm)	h_f (nm)	W_e (%)
Non-nitrided	4.7	234.3	197.7	15.7
	± 0.3	± 5.9	± 6.6	± 0.9
Nitrided	13.7	148.4	81.4	45.1
	± 0.75	± 3.8	± 4.2	± 1.6

loading/unloading rate: 1400 $\mu\text{N/s}$ maximum load: 7000 μN







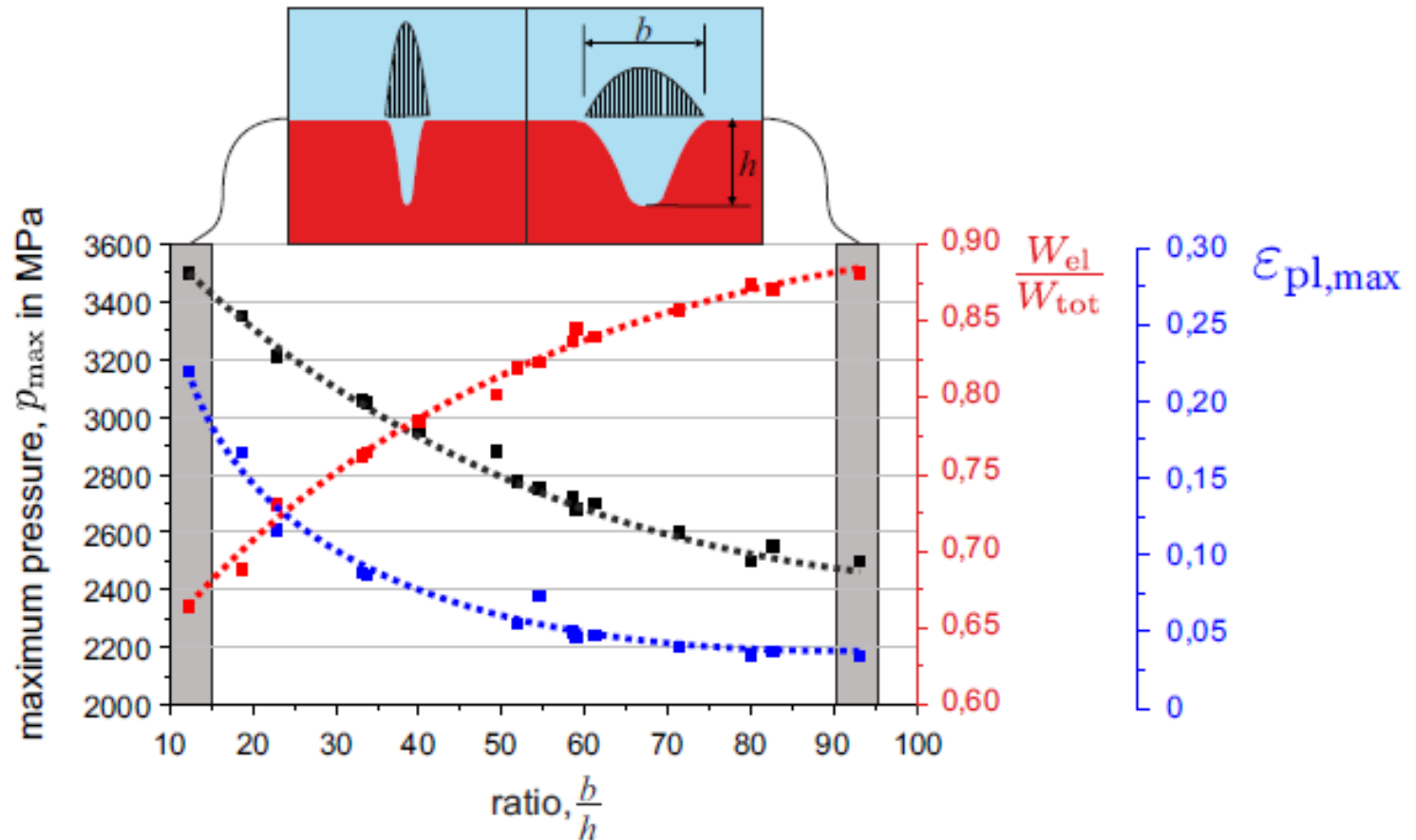


Figure 12: Relationship between maximum pressure p_{max} , ratio of elastic to total deformation energy $\frac{W_{el}}{W_{tot}}$, maximum plastic strain $\epsilon_{pl,max}$, and the ratio of pit width to pit depth $\frac{b}{h}$

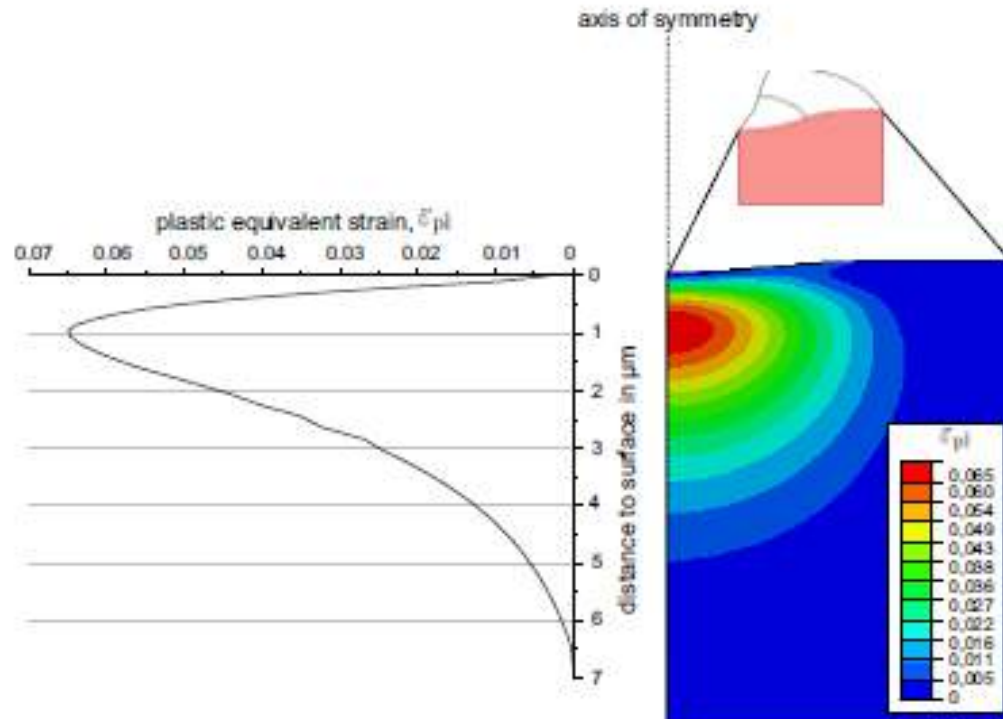


Figure 13: Calculated plastic strain distribution of a measured pit in copper with the profile of plastic strain strain along the axis of symmetry

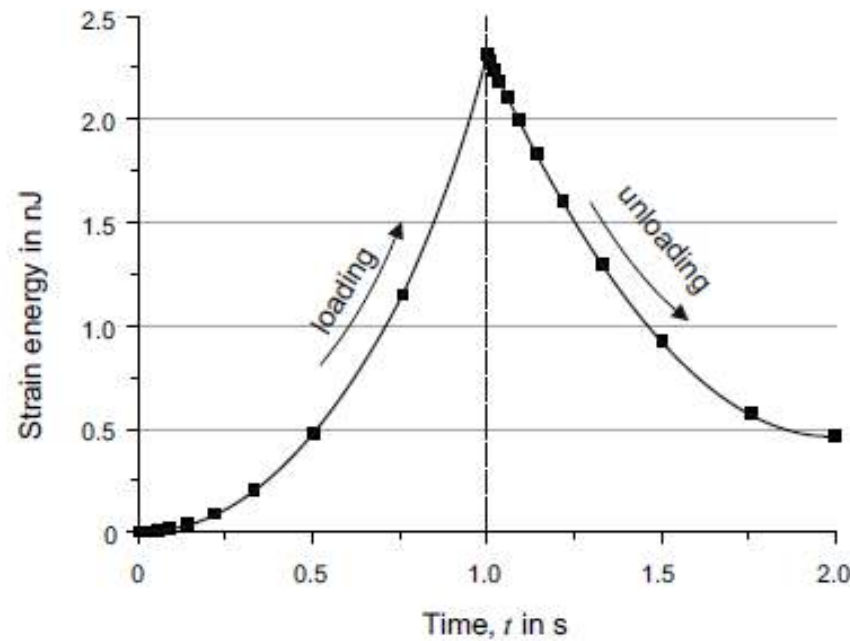


Figure 14: Strain energy of elastic and plastic deformation during loading and unloading

F. Pohl, S. Mottyll, R. Skoda, S. Huth - Evaluation of cavitation-induced pressure loads applied to material surfaces by finite-element assisted pit analysis and numerical investigation of the elasto-plastic deformation of metallic materials – to be published in *Wear*,

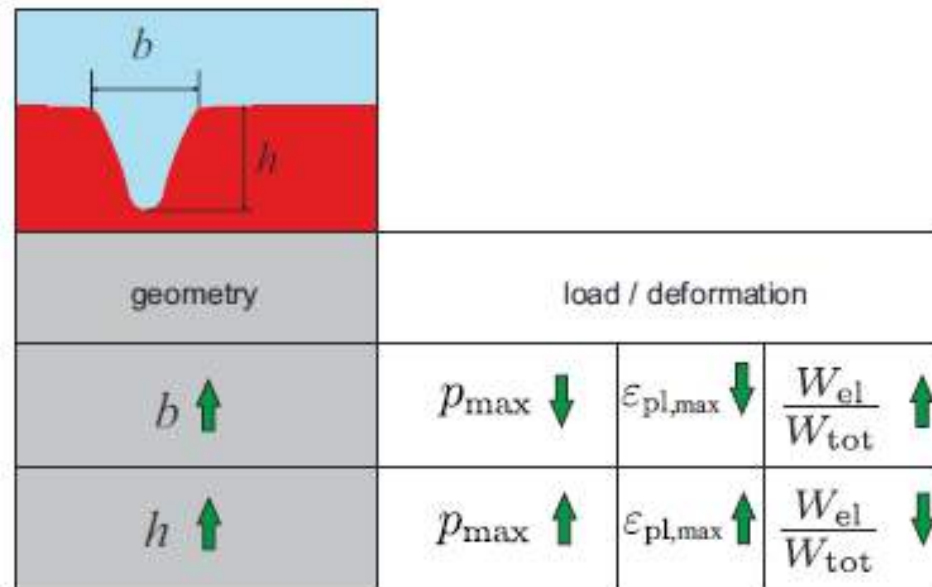
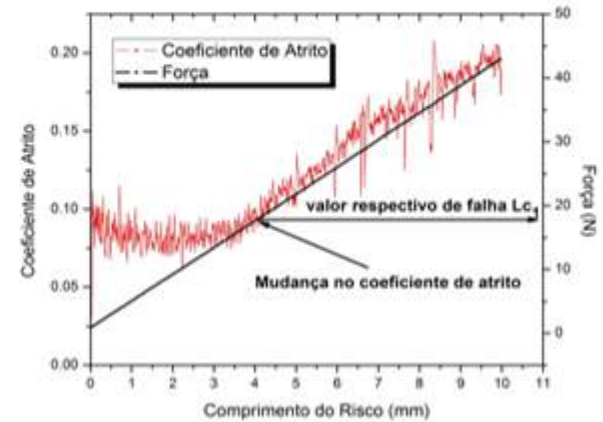
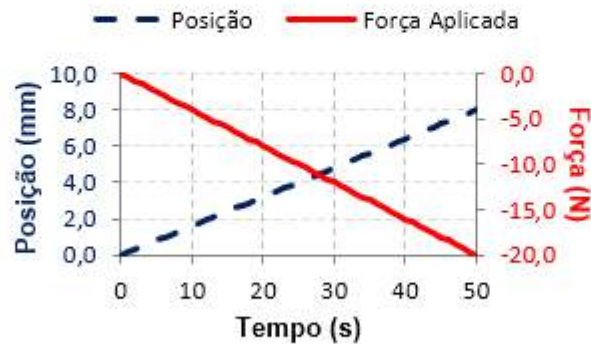


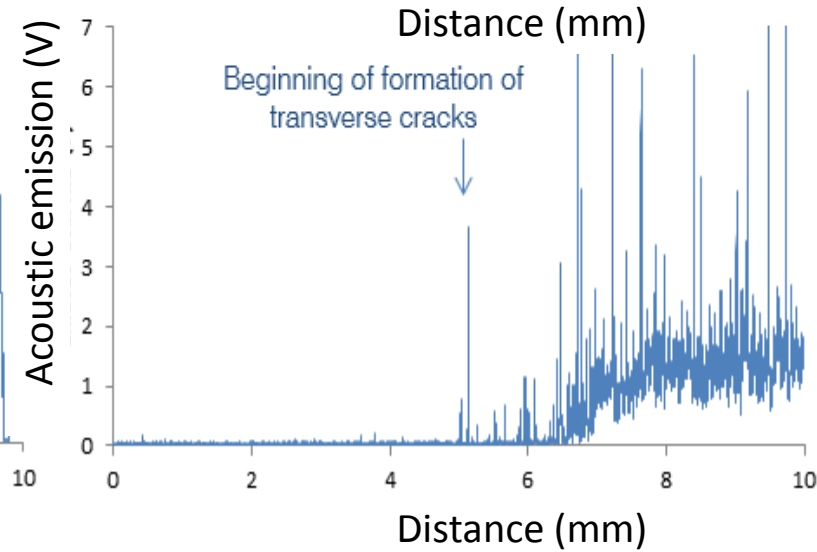
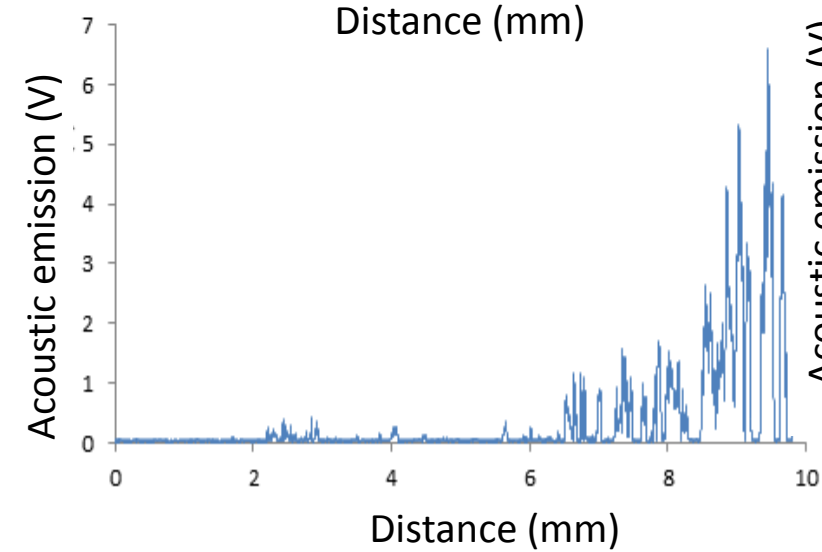
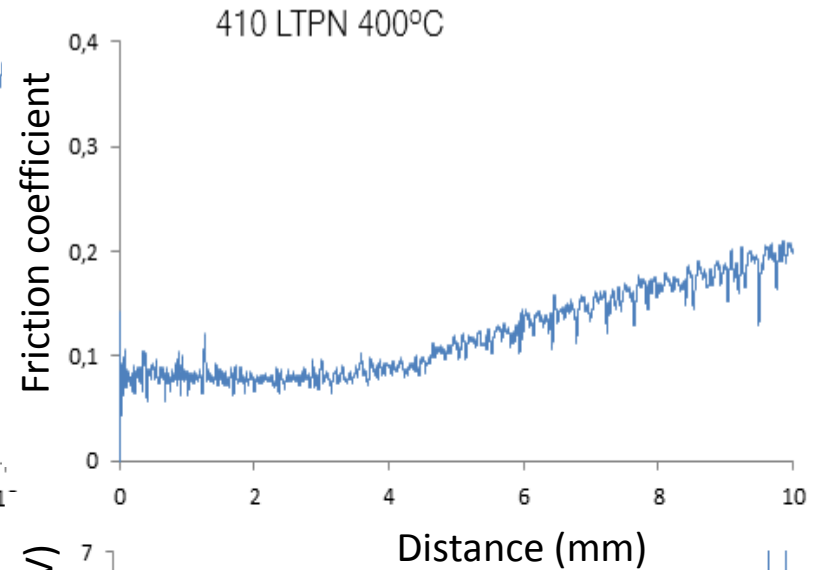
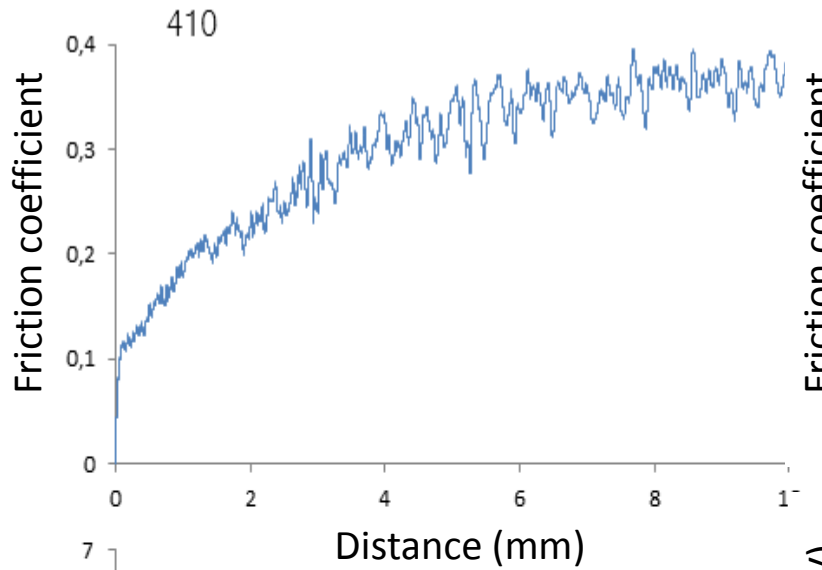
Figure 15: Summary of the relationships between the pit geometry (b and h) and the maximum pressure p_{\max} , the ratio of elastic to total deformation energy $\frac{W_{\text{el}}}{W_{\text{tot}}}$, and the maximum plastic strain $\varepsilon_{\text{pl,max}}$

Instrumented Linear Scratch Tests

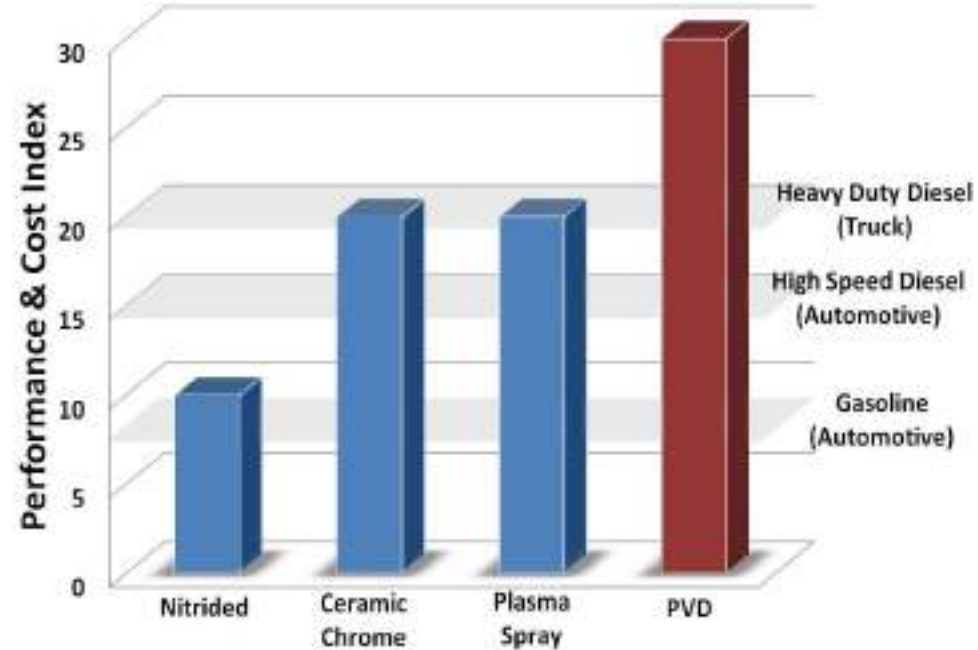
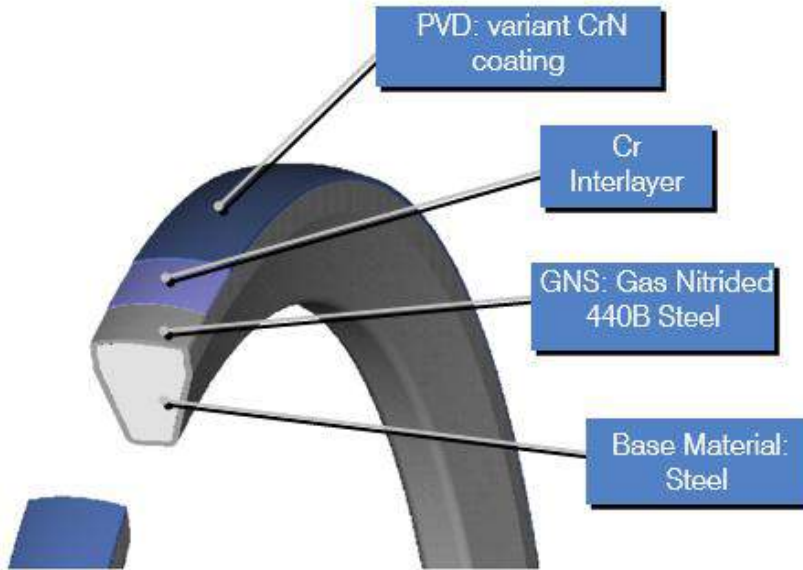


- Abrasive wear due to scratching using a diamond tip
- Measuring COF – Coefficient of friction

N Expanded Martensite



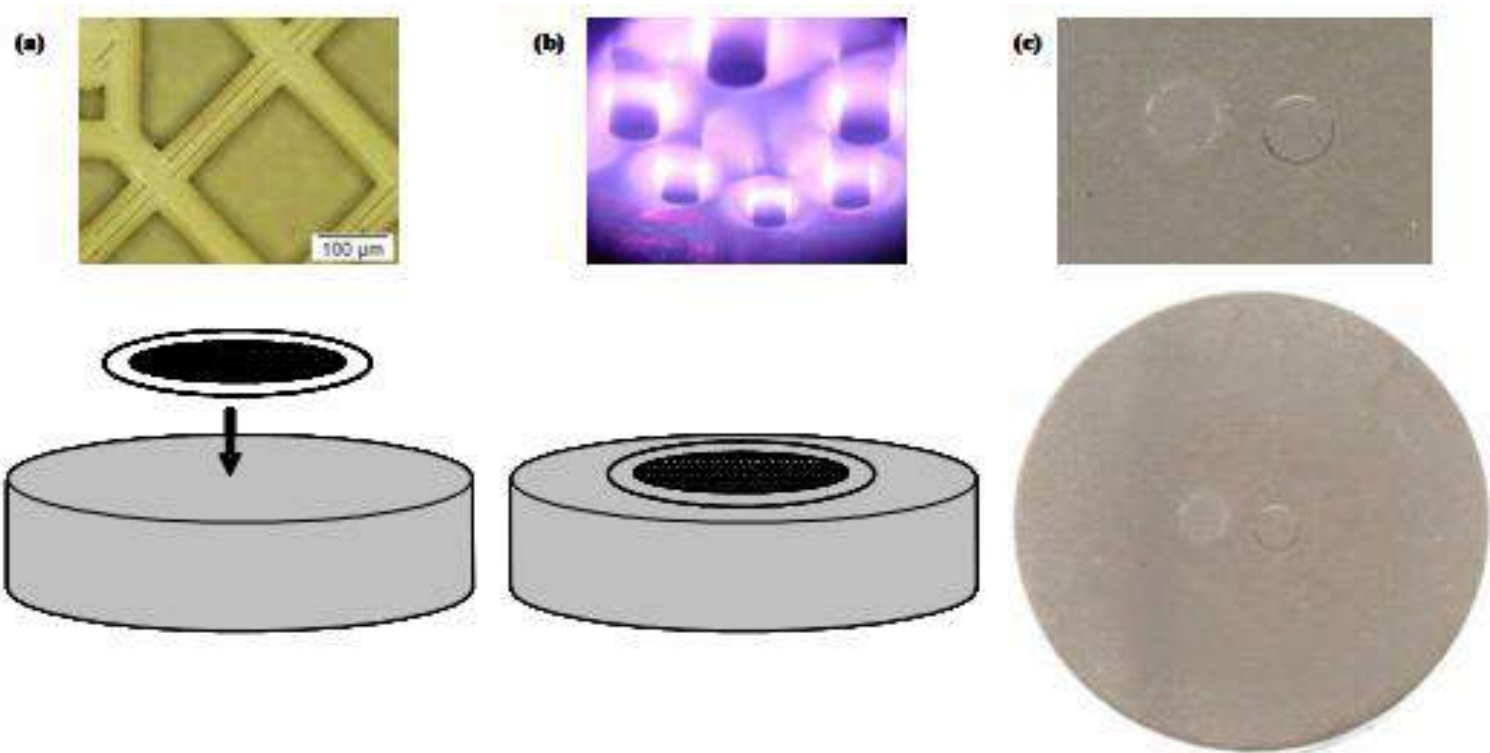
Duplex Coating of Martensitic 440B Stainless Steel



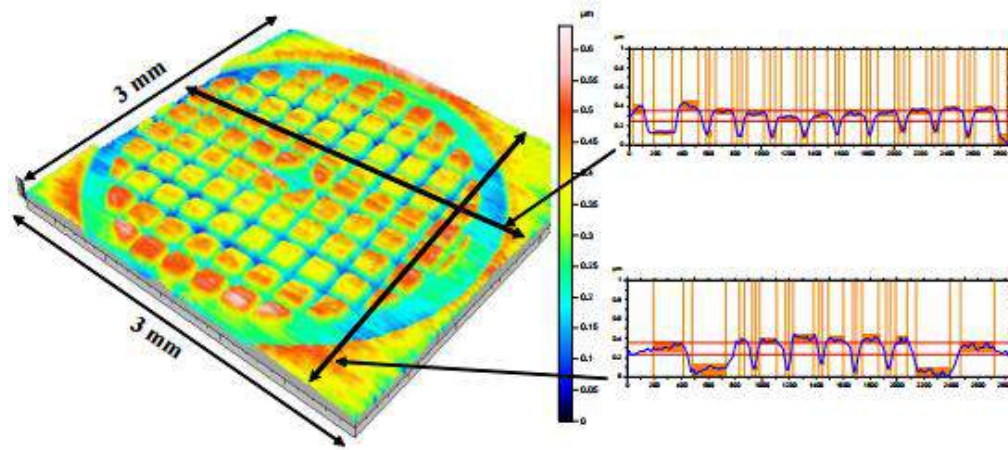
5

EDMM - Materials Science, Juliano Araujo, April - 2010

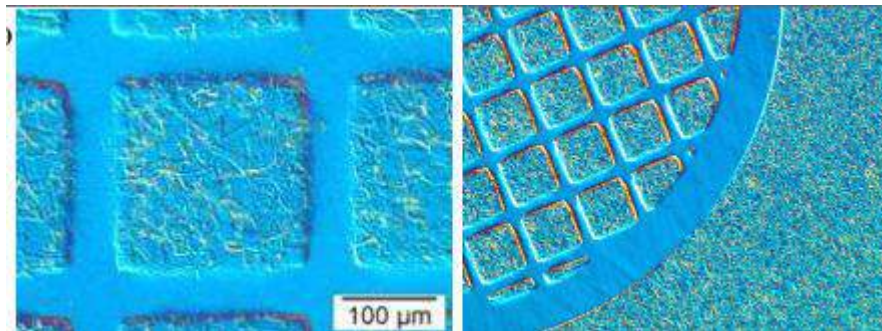
- ✓ PVD coatings has been increasingly employed on piston rings:
 - Excellent wear resistance
 - Small wear of cylinder
 - High scuffing resistance and low friction coefficient.

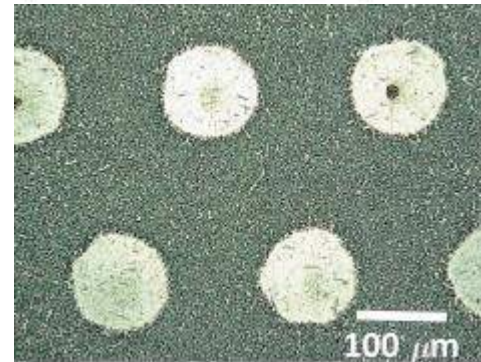
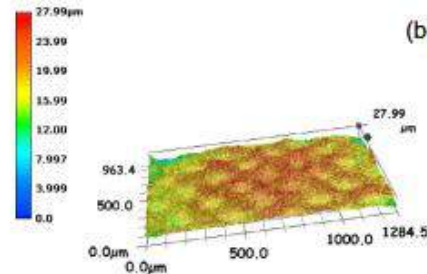
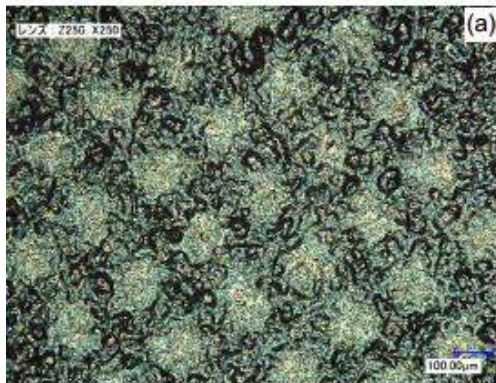
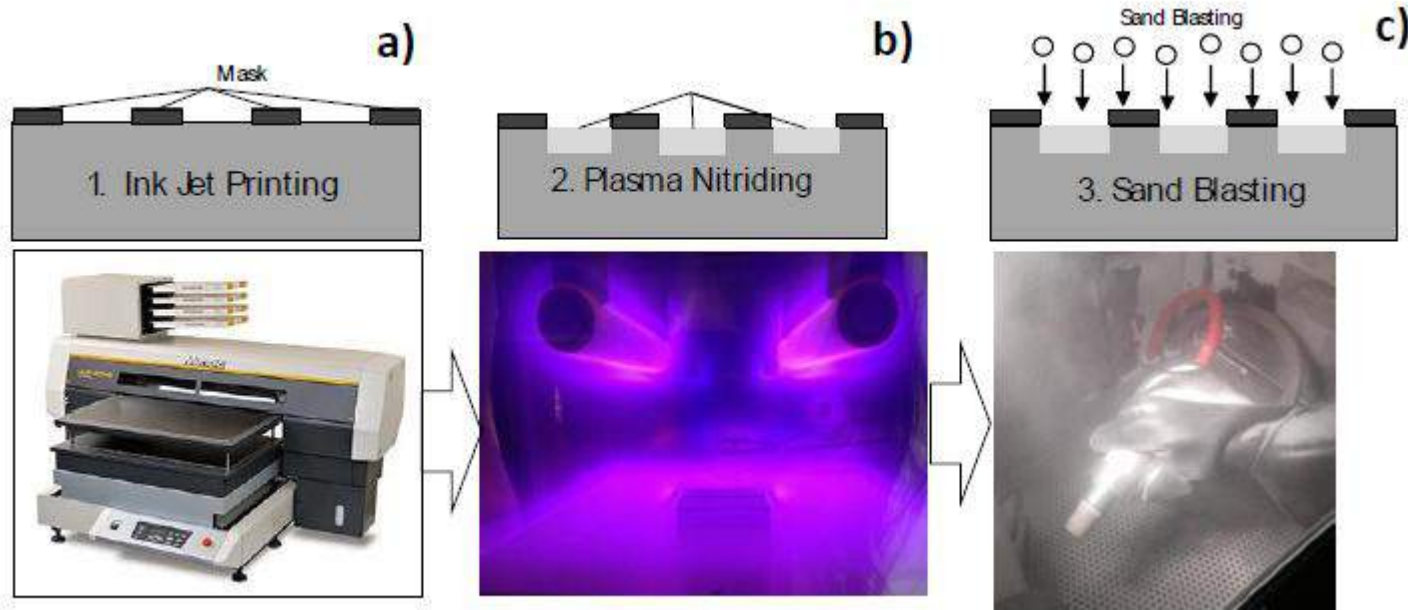


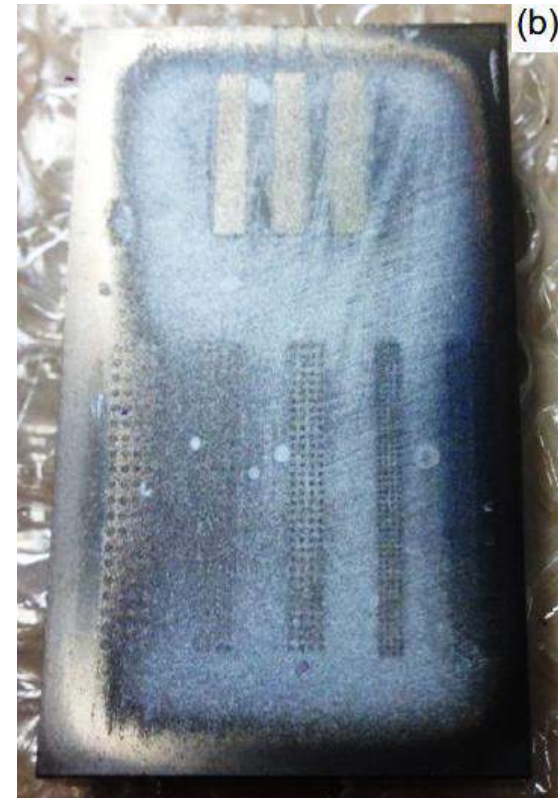
- Expansion of austenite occurs horizontally and vertically
- Vertical expansion is responsible for the patterning



- Expansion of austenite occurs horizontally and vertically
- Vertical expansion is responsible for the patterning







- The tribological behavior of stainless steels can be improved by using plasma assisted thermochemical treatments.
- Depending on the contact stresses the duplex and combined treatments HTGN, LTPN and PVD–TiN may be used to obtain a better combination of surface properties.
- Low temperature plasma treatments lead to the formation of supersaturated metastable phases on the surface (expanded austenite, expanded ferrite and expanded martensite) increasing hardness, wear resistance and cavitation-erosion resistance.
- The expanded phases show very low coefficient of friction when scratched with a diamond tip during instrumented scratch testing.
- Microtexturing and Surface Patterning can be accomplished by plasma assisted surface treatment.

ACKNOWLEDGEMENTS

- Fundação de Amparo à Pesquisa do Estado de São Paulo (FAPESP)
- Prof. Hanshan Dong - University of Birmingham – Surface Engineering Group
- Dr. Xiao-Ying Li - University of Birmingham – Surface Engineering Group
- Carlos Eduardo Pinedo – Heat Tech – Technologies for Heat Treatment and Surface Engineering
- Pró-Reitoria de Pesquisa da USP
- Luis Armando Espitia
- Luis Bernardo Varela
- Fernando Luis Sato
- Dairo Hernan Mesa
- Sharys Varela
- Abel André Cândido Recco
- Diana Maria López
- Carlos Mario Garzón
- Claudia Patrícia Ossa
- Alejandro Toro
- Juan Manuel Vélez



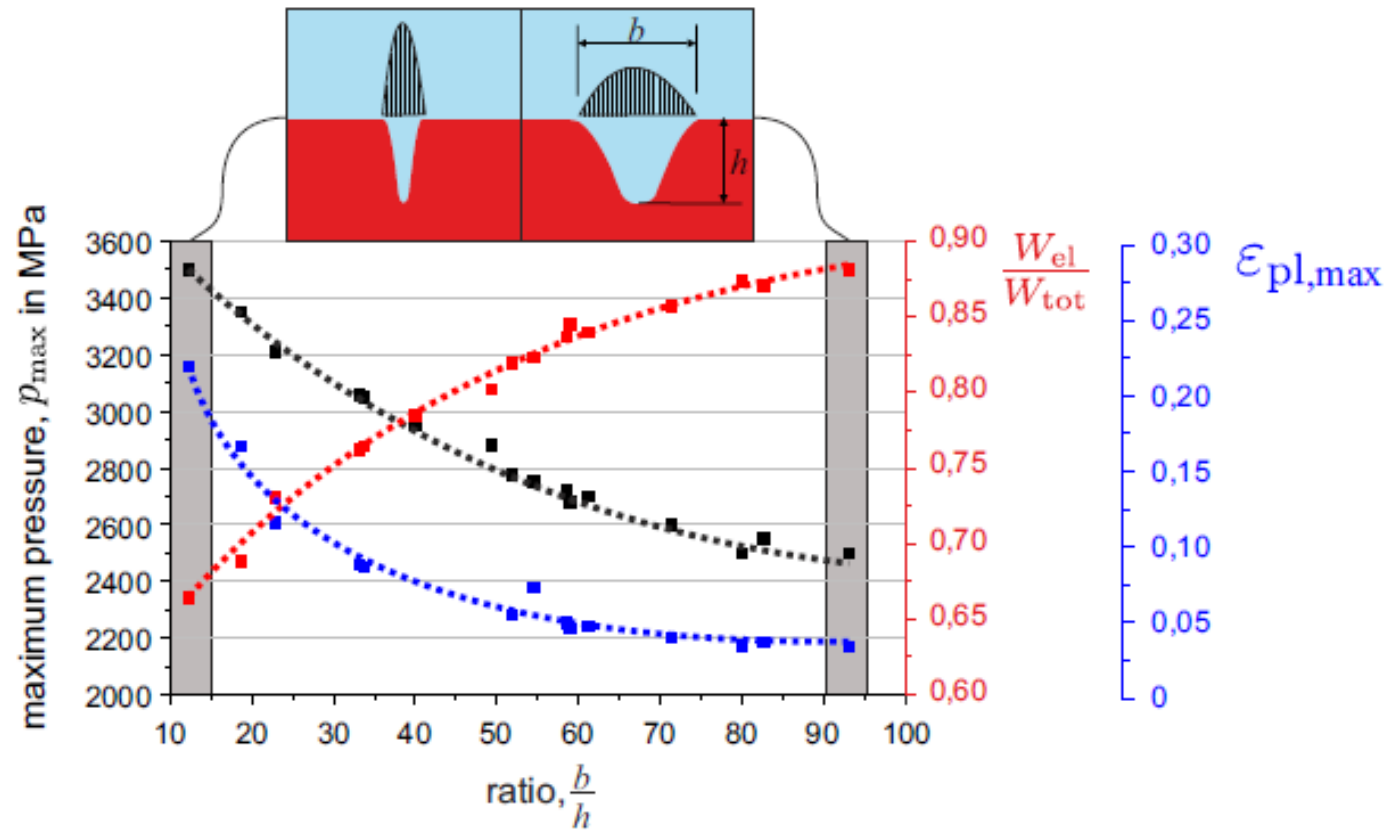


Figure 12: Relationship between maximum pressure p_{max} , ratio of elastic to total deformation energy $\frac{W_{el}}{W_{tot}}$, maximum plastic strain $\epsilon_{pl,max}$, and the ratio of pit width to pit depth $\frac{b}{h}$

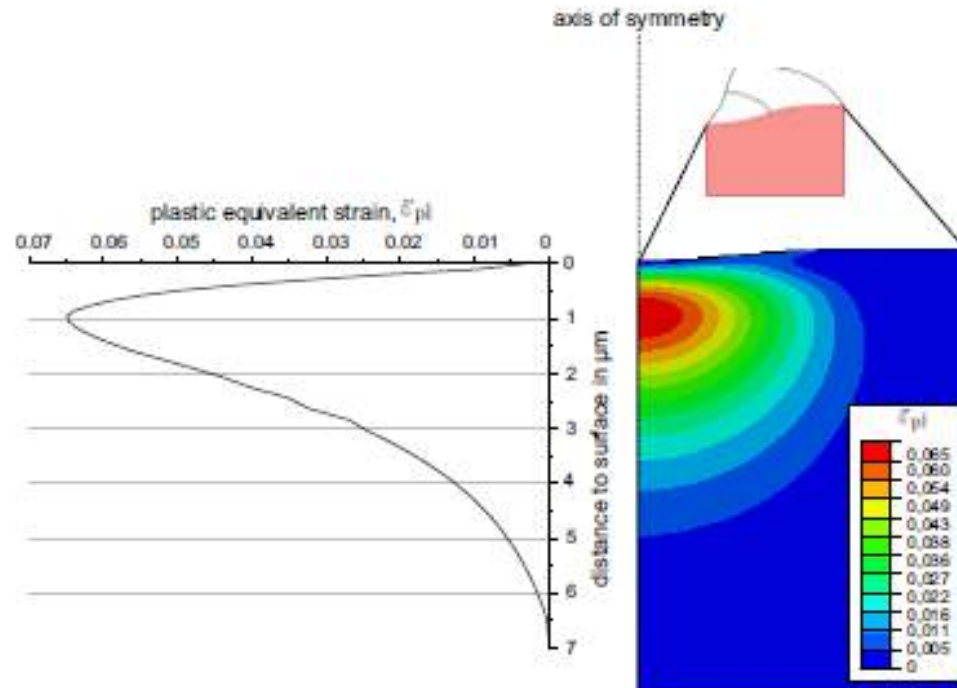


Figure 13: Calculated plastic strain distribution of a measured pit in copper with the profile of plastic strain strain along the axis of symmetry

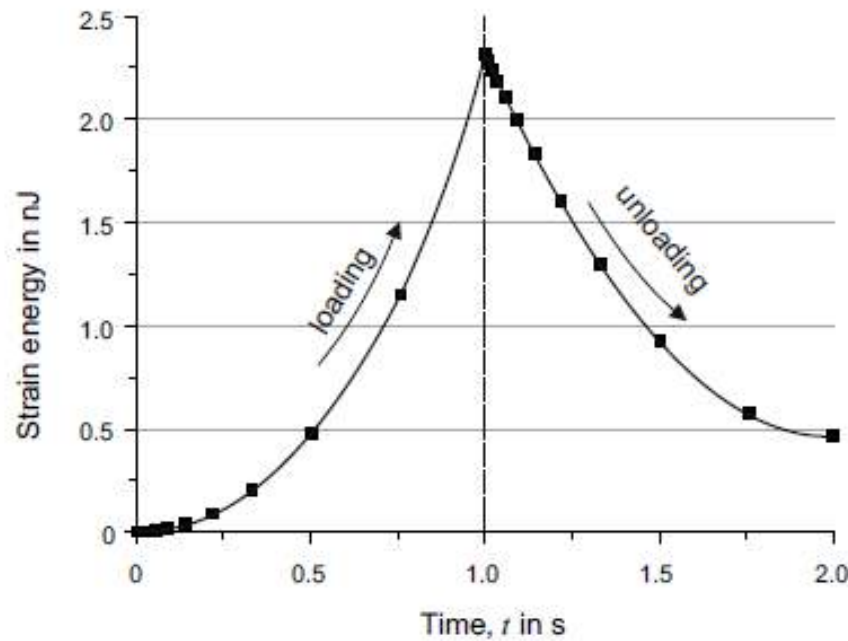


Figure 14: Strain energy of elastic and plastic deformation during loading and unloading

F. Pohl, S. Mottyll, R. Skoda, S. Huth - Evaluation of cavitation-induced pressure loads applied to material surfaces by finite-element assisted pit analysis and numerical investigation of the elasto-plastic deformation of metallic materials – to be published in *Wear*,

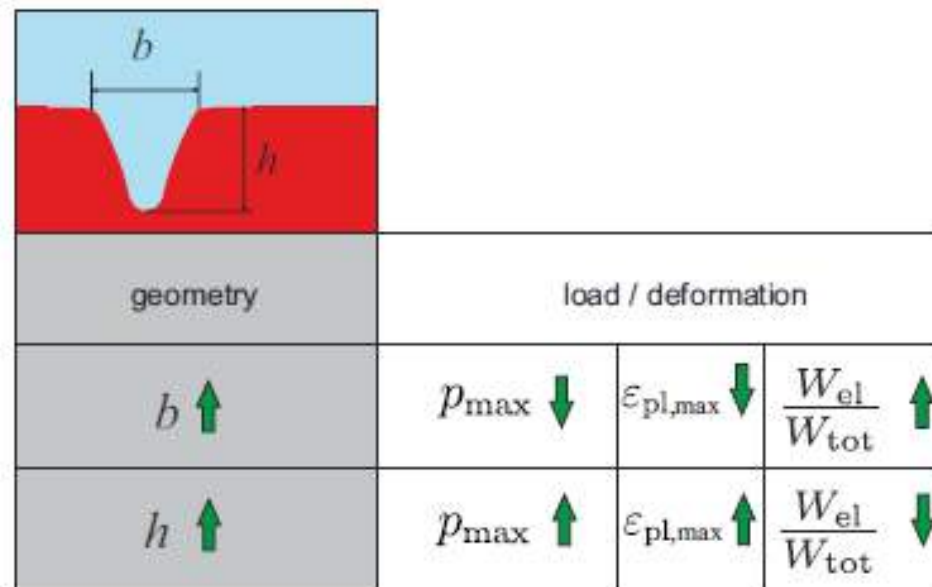


Figure 15: Summary of the relationships between the pit geometry (b and h) and the maximum pressure p_{\max} , the ratio of elastic to total deformation energy $\frac{W_{\text{el}}}{W_{\text{tot}}}$, and the maximum plastic strain $\varepsilon_{\text{pl,max}}$